Frentes

- Definição
- Tipos de frentes
- Dinâmica de uma pluma
- Equilíbrio dinâmico
- Efeito do vento e da maré

Frentes

- Regiões oceânicas onde águas de características diversas se encontram:
  - Larga escala – FST, FP
  - Meso-escala – FSTP
  - Micro-escala – frentes estuarinas

Tipos de frentes de plataforma

- Frentes de quebra de plataforma – Talude-Argentina, FSTP
- Frentes de ressurgência
- Frentes de marés – Patagônia (Península Valdez)
- Frentes de rios
- Frentes de estuários

Frentes

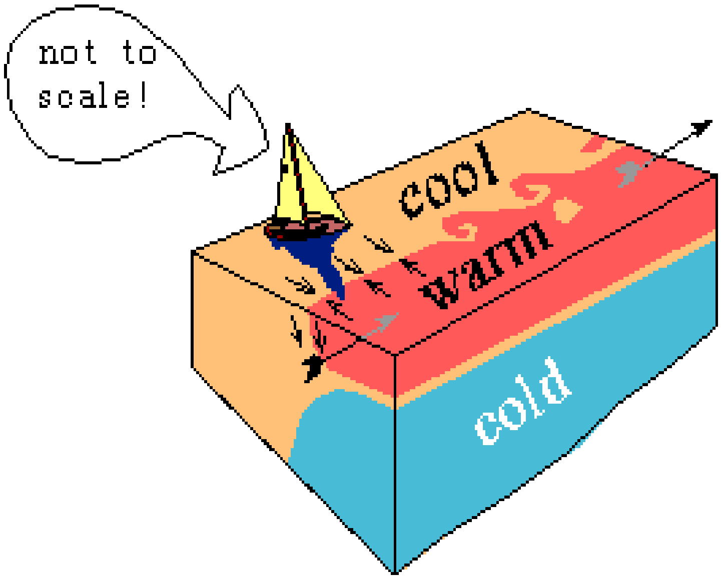
not to
scale!
cool
warm
cold

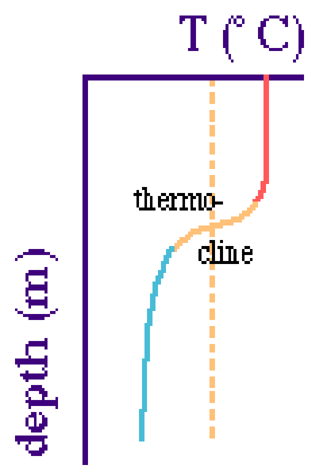
T (° C)
thermo-
cline
depth (m)

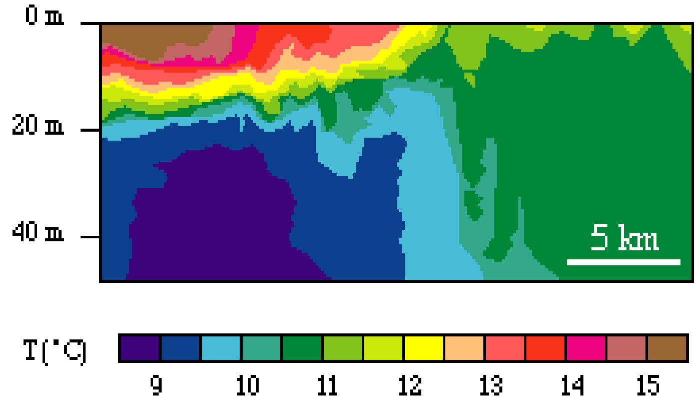
0 m
20 m
40 m
5 km
T(°C)
9
10
11
12
13
14
15

Tipos de frentes

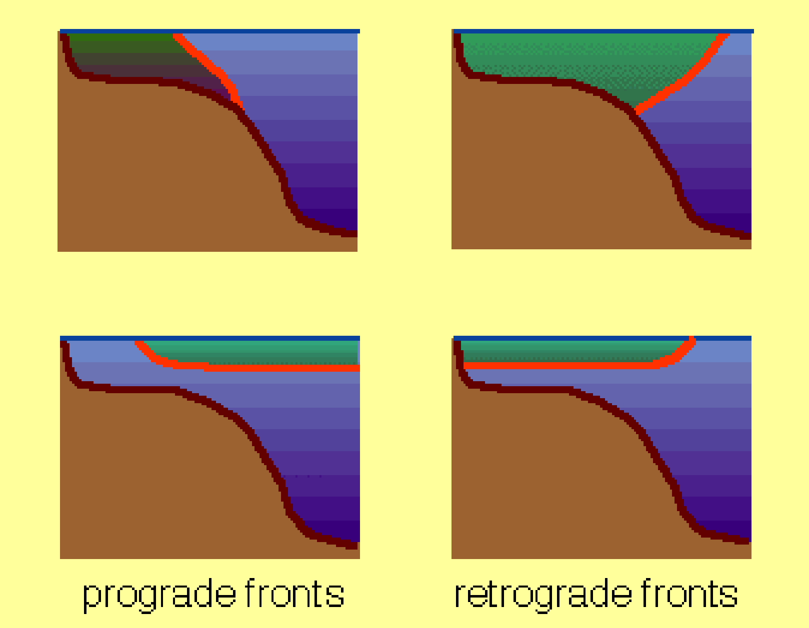

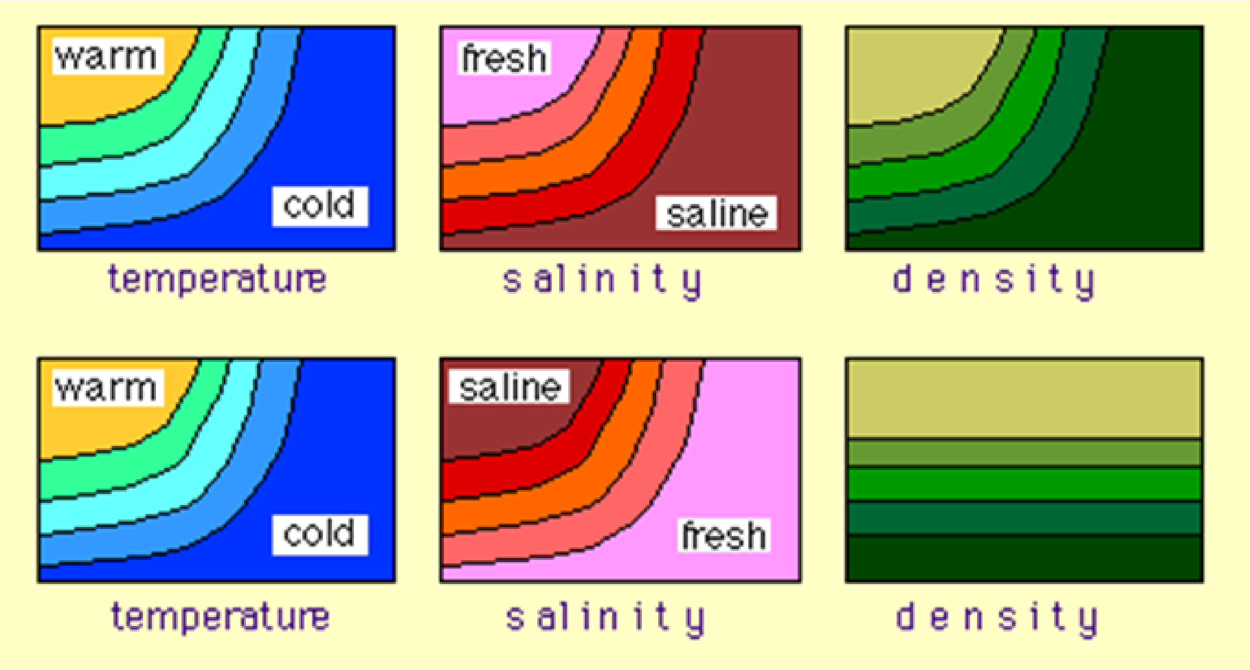


Movimentos através de uma frente

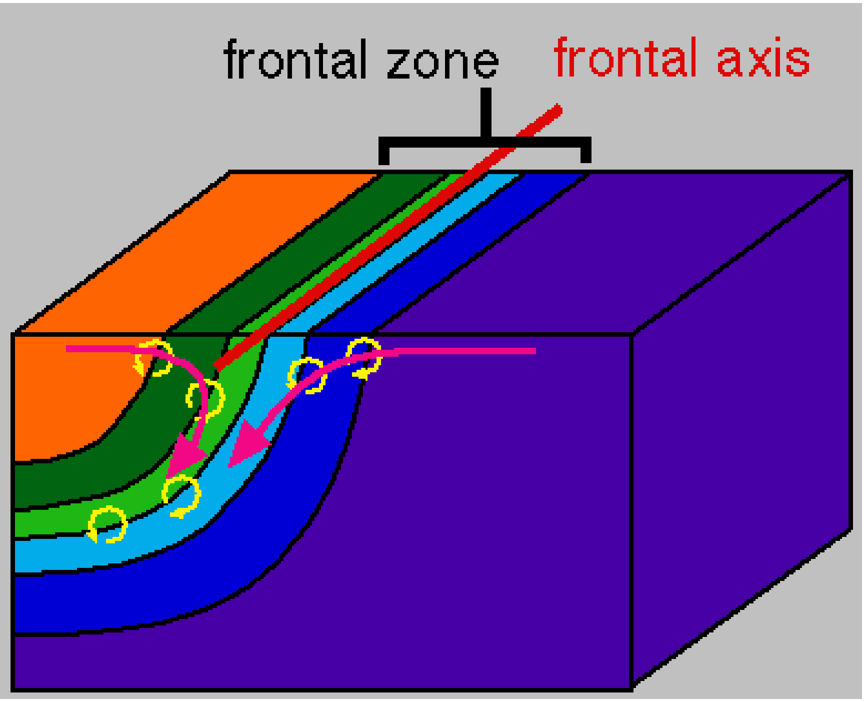

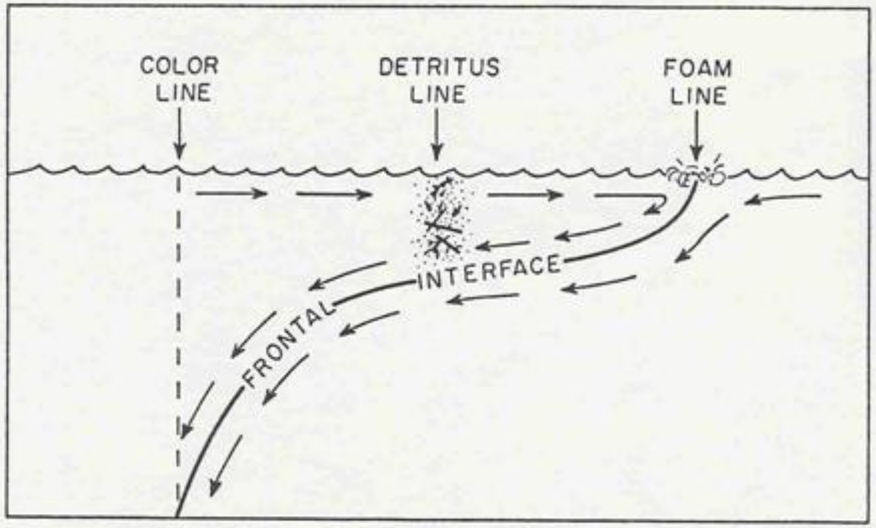

FIGURE 15. Schematic cross section of a shallow front. Three boundaries are often visible:

1. The color front perceived to lie where the depth integrated upwelled light undergoes a distinct spectral shift in the region of rapidly descending isopycnals.
2. The detritus line where large buoyant objects are trapped by oppositely directed currents at the surface and near the frontal interface.
3. The foam line which is located at the surface convergence. Since the frontal slope may be $\sim 10^{-2}$, the three demarcations can be separated by several tens of meters.[8,48]

Frentes de plataforma

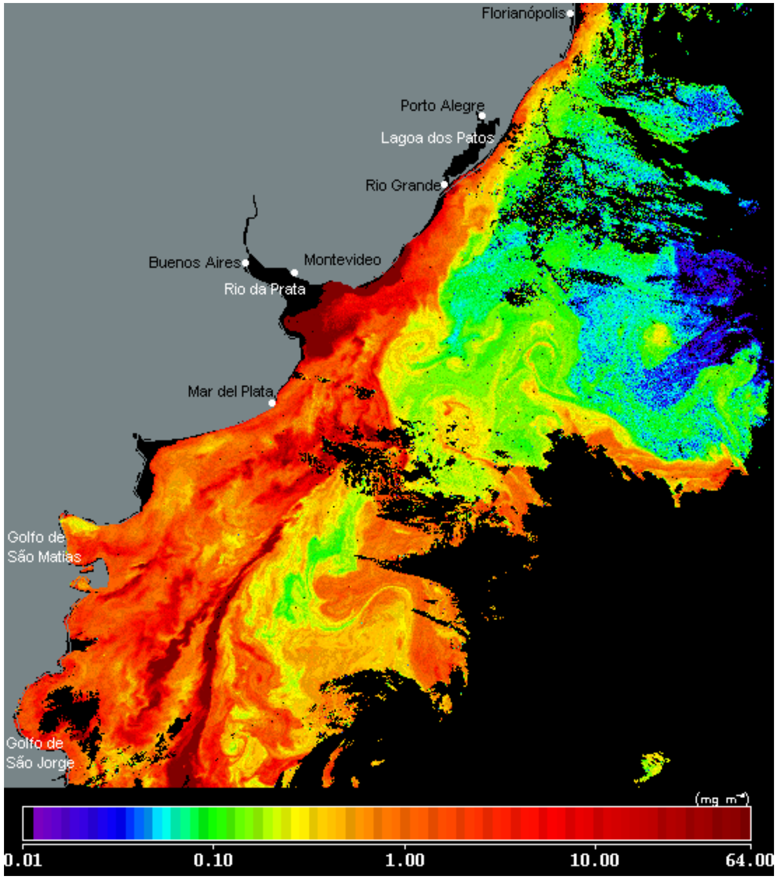

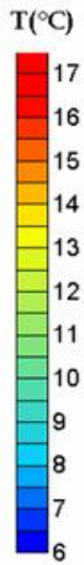

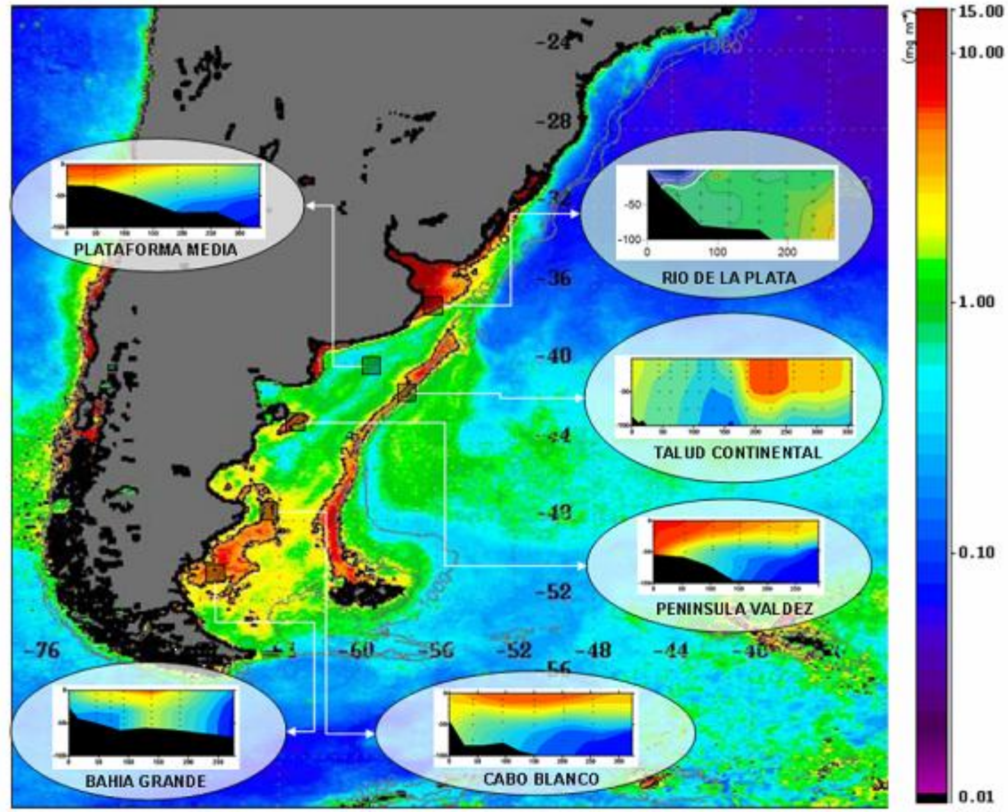

Figura 2-1 CSAT verano. Identificación de frentes

As frentes

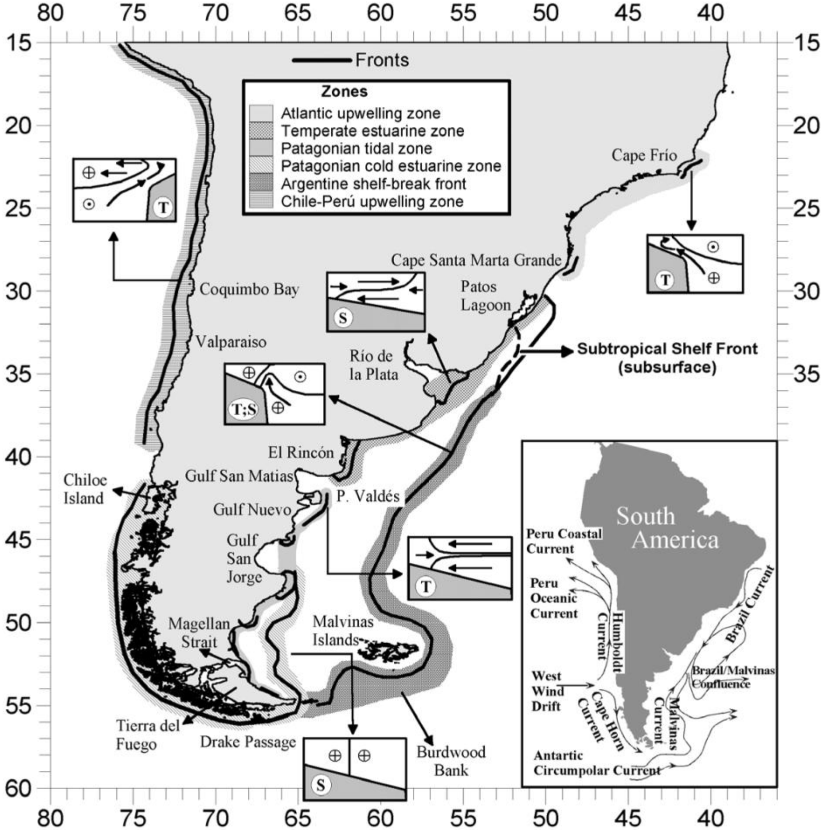

Acha et al. (2004)

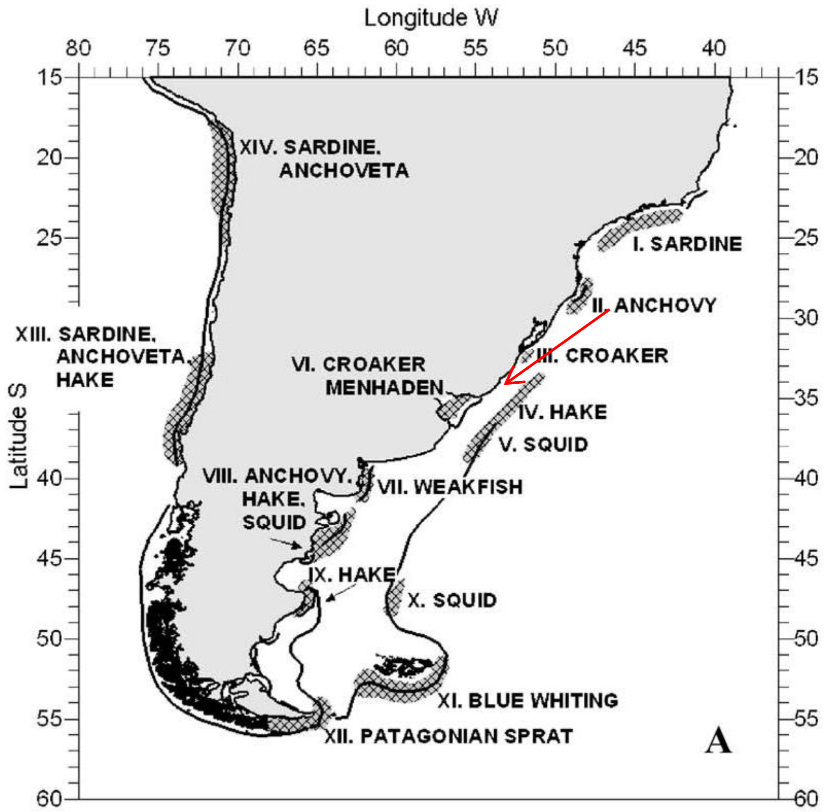

Frentes de Plataforma

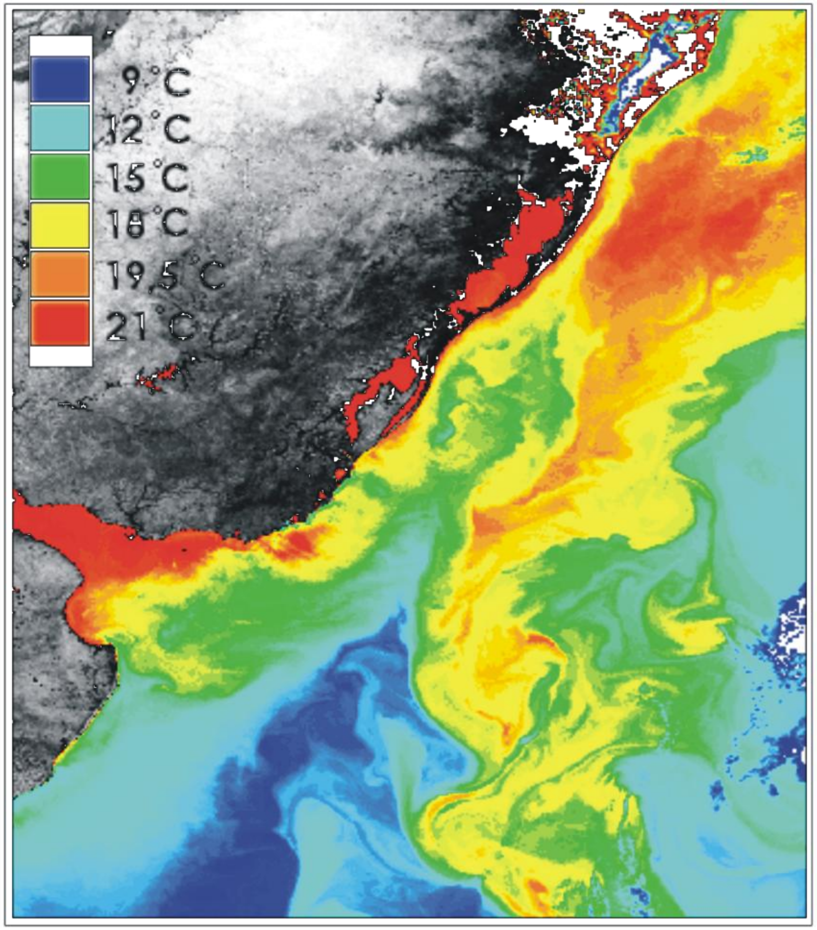

Frente de quebra de plataforma

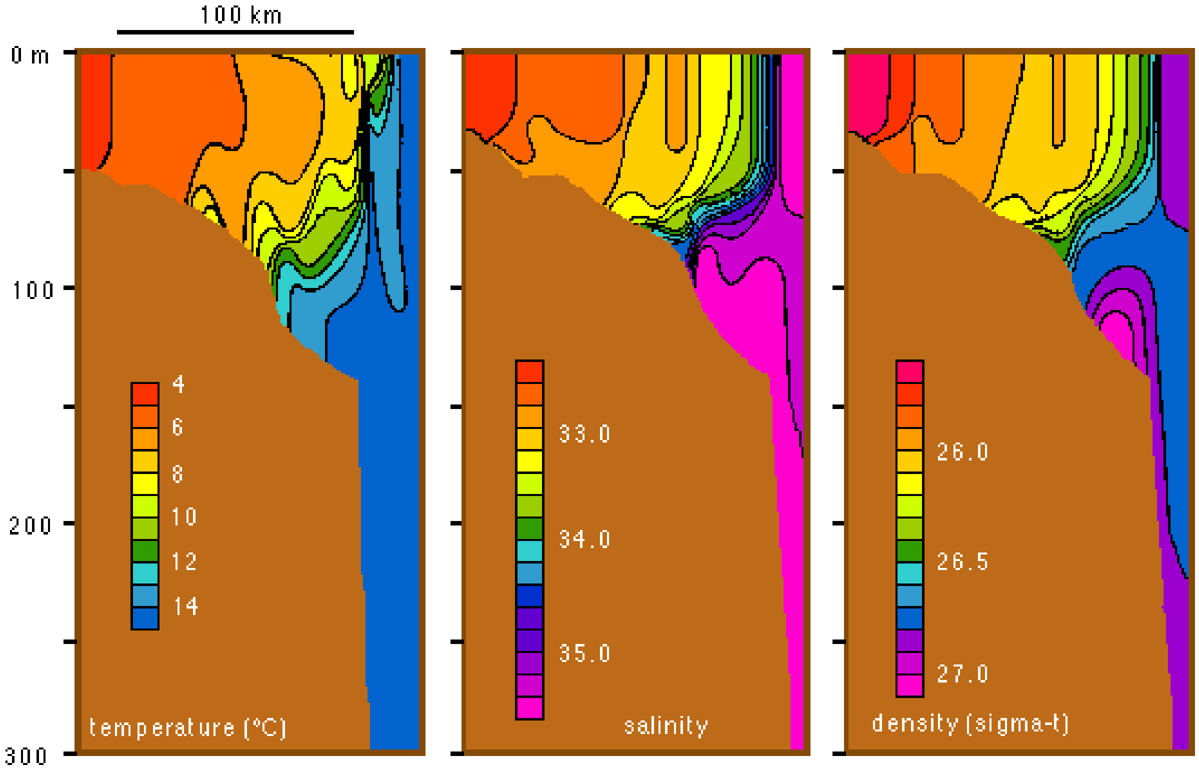

Frente de Talude - Argentina

Figura 2-25 Imagen satelital nocturna de poteros en el TC

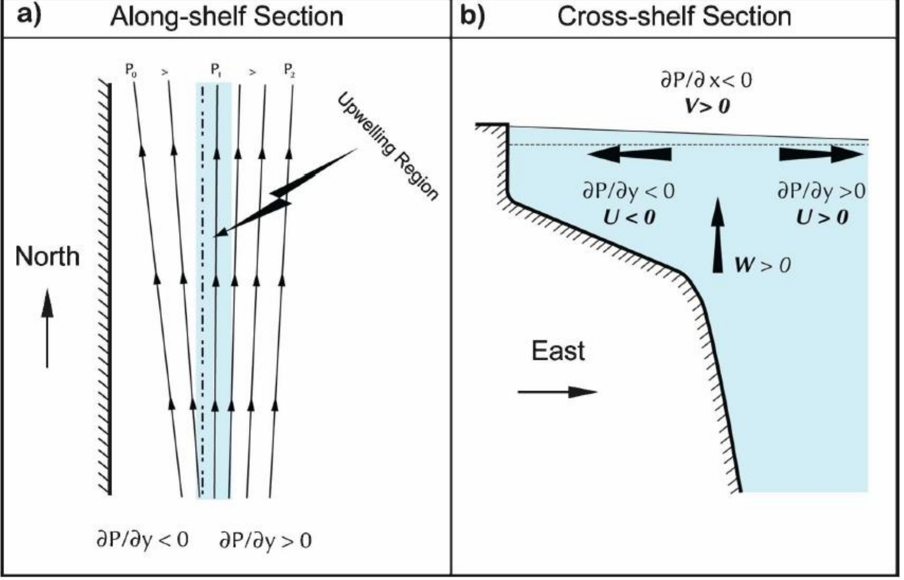

FIG. 2. Schematic representation of the development of shelfbreak upwelling by a cyclonic current. (a) The downstream spreading of the streamfunction associated with the slope current. The dotted line marks the position of the shelf break. A small portion of the downwelling current spreads onto the shelf while its axis shifts toward deep waters. This diverging motion generates downstream pressure gradients of opposite signs at each side of the shelfbreak. (b) The cross-shelf circulation patterns associated with this diverging motion.

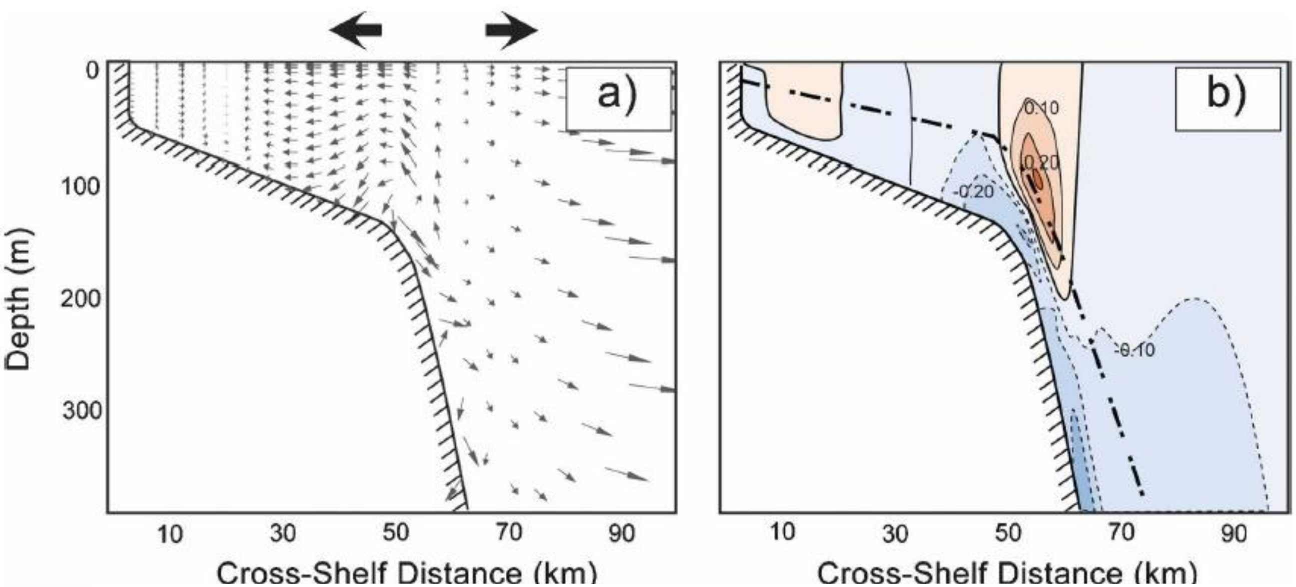

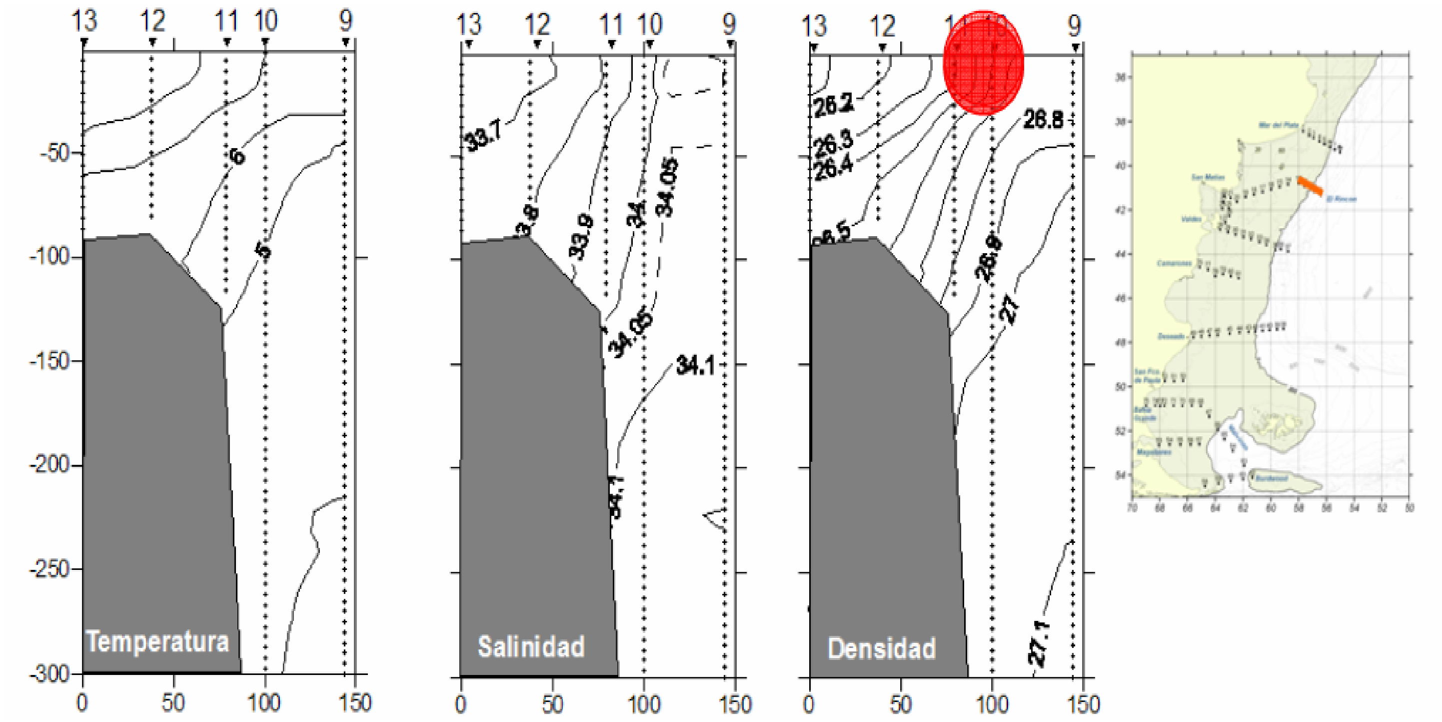

Figura 5-15 Secciones de temperatura, salinidad y densidad transversales al talud entre 40 y 41°S

Secciones de temperatura, salinidad y densidad transversales al talud entre 40 y 41°S. Corresponden al día 10 de octubre de 2005. Pierna El Rincón. El círculo sombreado en rojo destaca la posición del frente en superficie. La sección de densidad muestra la superficialización de las superficies isopicnicas entre los valores de sigma 26,4 y 26,7 Kg m^{-3} en las estaciones 10 y 11 que son indicativas del frente TC

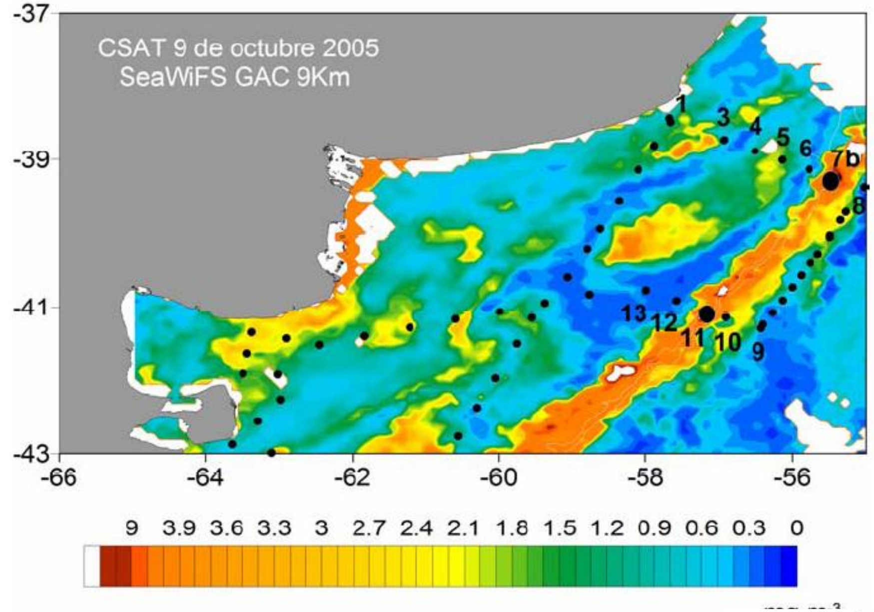

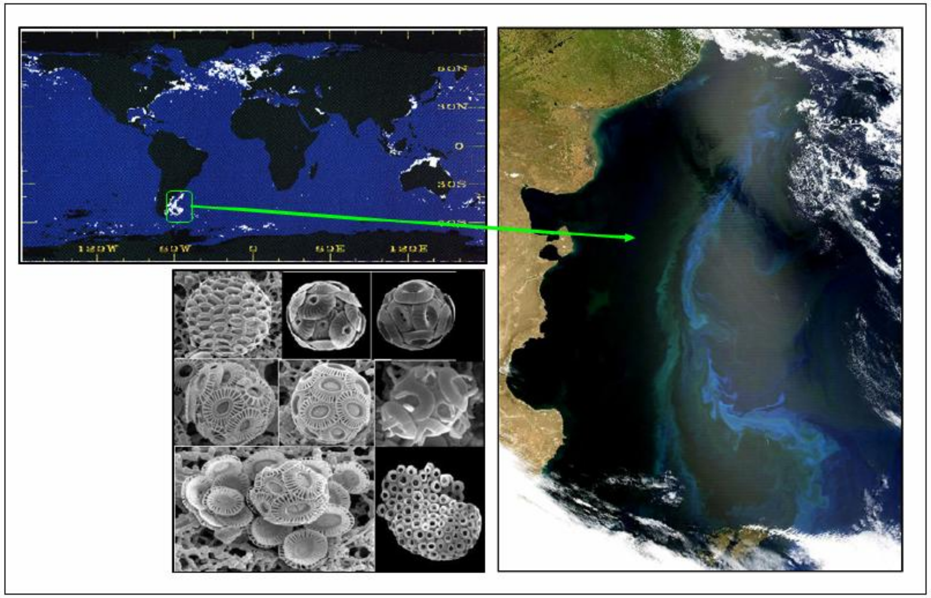

Figura 2-24 Concentraciones de cocolitofóridos imagen color real

Figura extraída del trabajo Garcia y otros (2006). En el panel superior izquierdo se muestran las concentraciones globales estimadas de cocolitofóridos (Brown y otros, 2000). Se destacan elevadas concentraciones en el Atlántico Sudoccidental. Panel inferior izquierdo: fotografías detalladas de caparazones microscópicos de calcita de distintas especies de cocolitofóridos. Panel derecho: Imagen SeaWiFS de color real que muestra la banda de alta reflectividad en las proximidades del talud continental argentino.

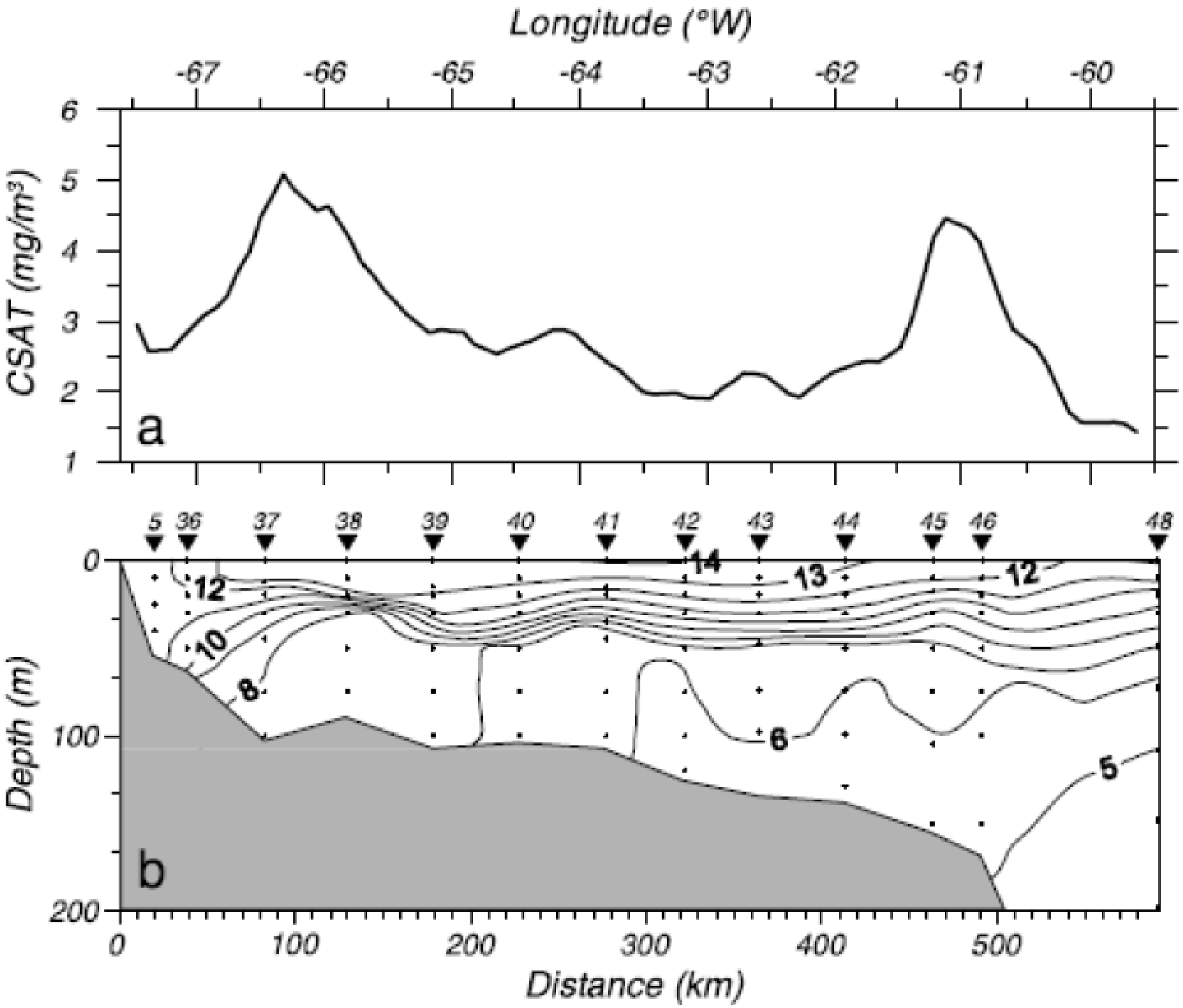

Figura 5-32 Sección temperatura transversal al talud BG

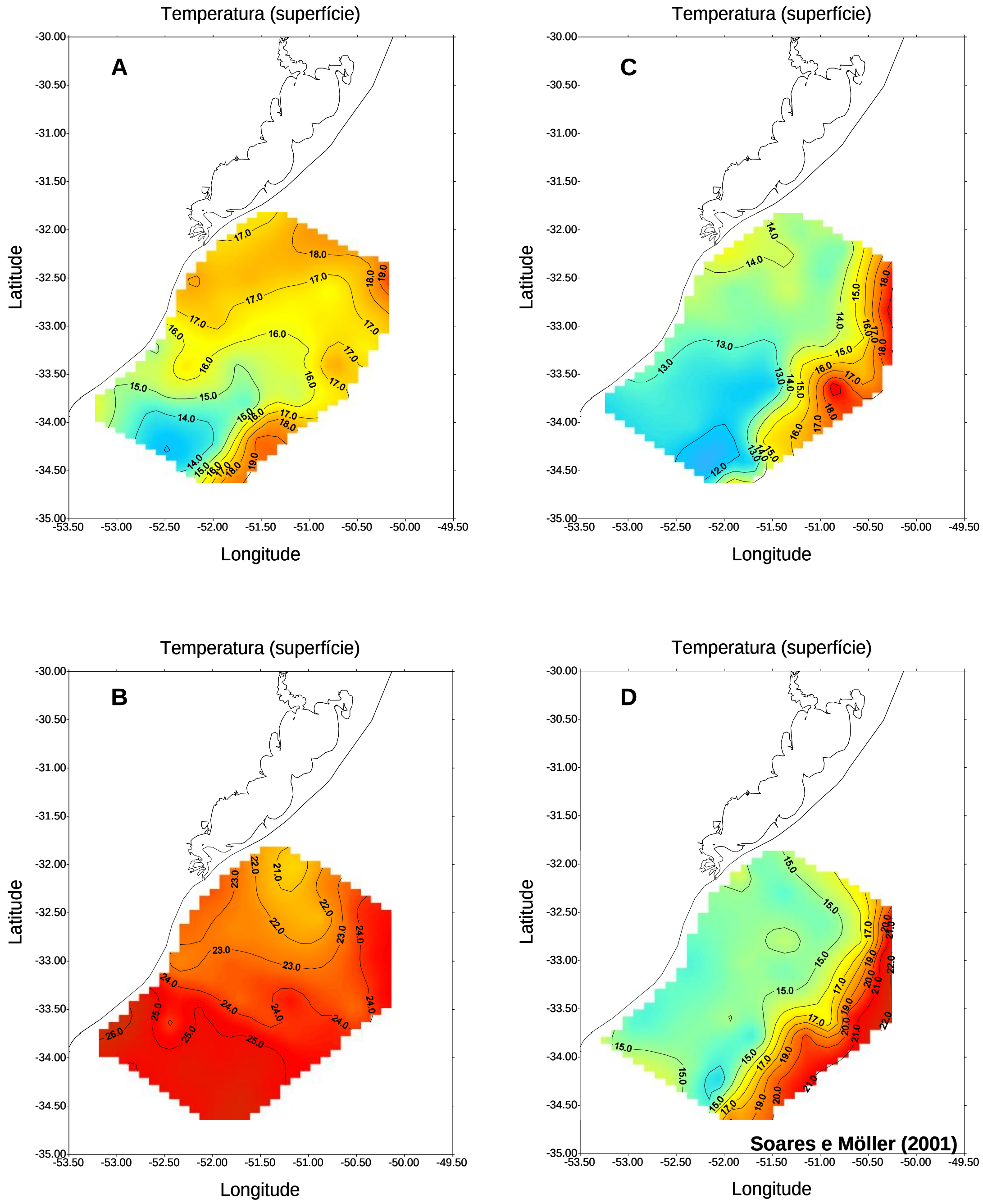
Temperatura (superfície)
A
Latitude
Longitude
Temperatura (superfície)
C
Latitude
Longitude
Temperatura (superfície)
B
Latitude
Longitude
Temperatura (superfície)
D
Latitude
Longitude
Soares e Möller (2001)

FSTP

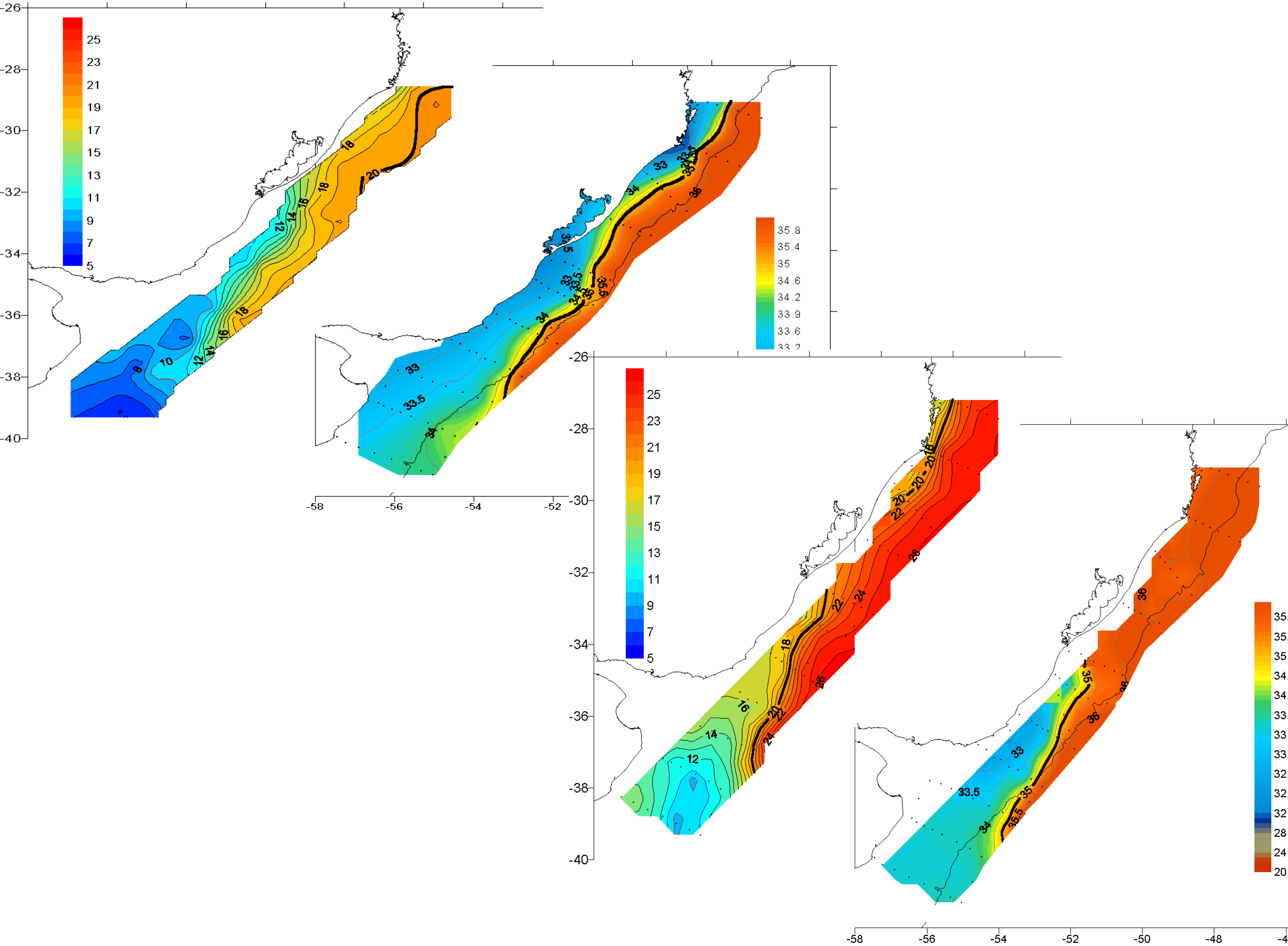

-26
-28
-30
-32
-34
-36
-38
-40
25
23
21
19
17
15
13
11
9
7
5
35.8
35.4
35
34.6
34.2
33.9
33.6
-58
-56
-54
-52
-50
-48

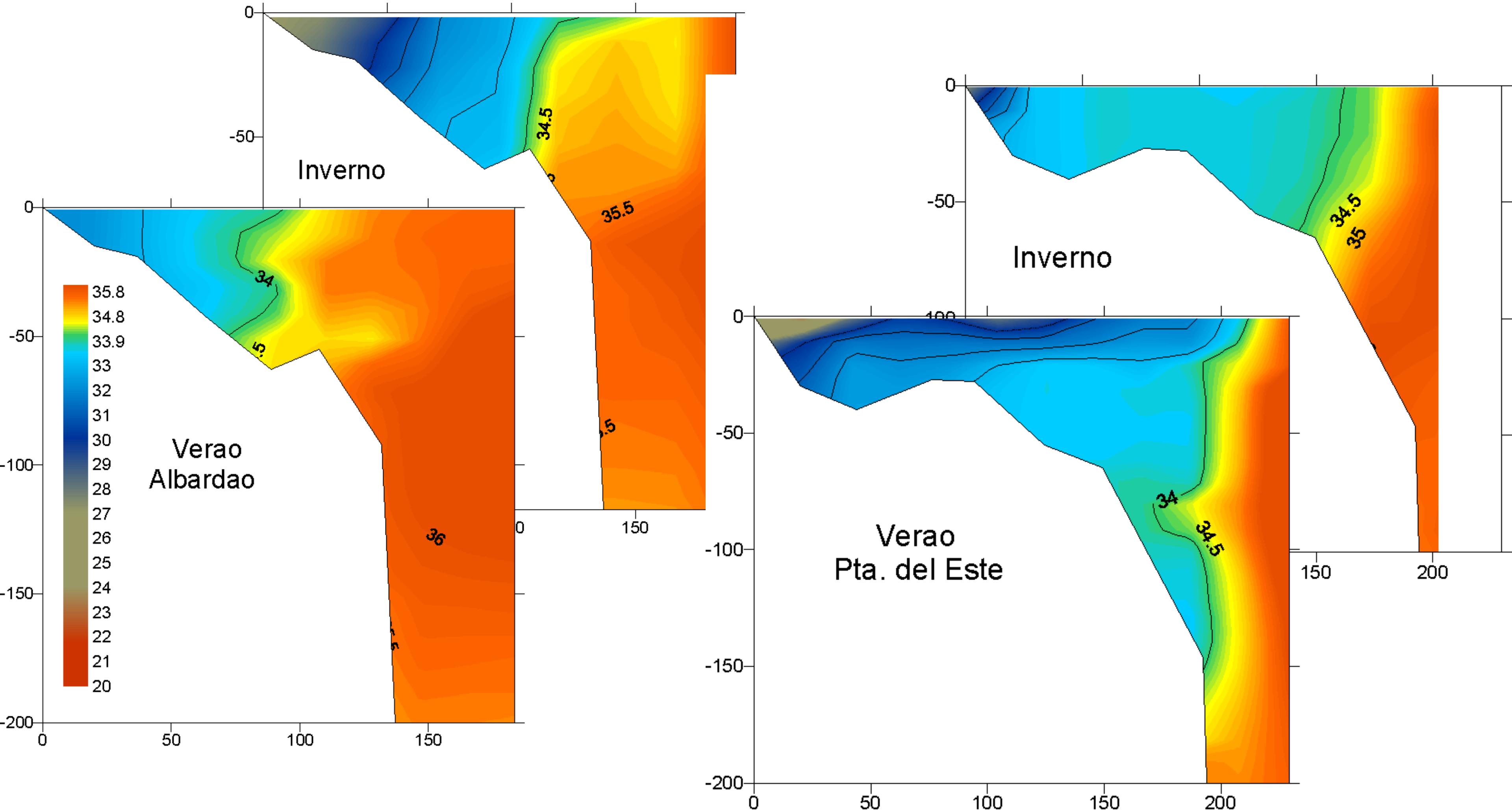
Inverno
Verao
Albardao
Inverno
Verao
Pta. del Este
35.8
34.8
33.9
33
32
31
30
29
28
27
26
25
24
23
22
21
20
34.5
35.5
34
36
35

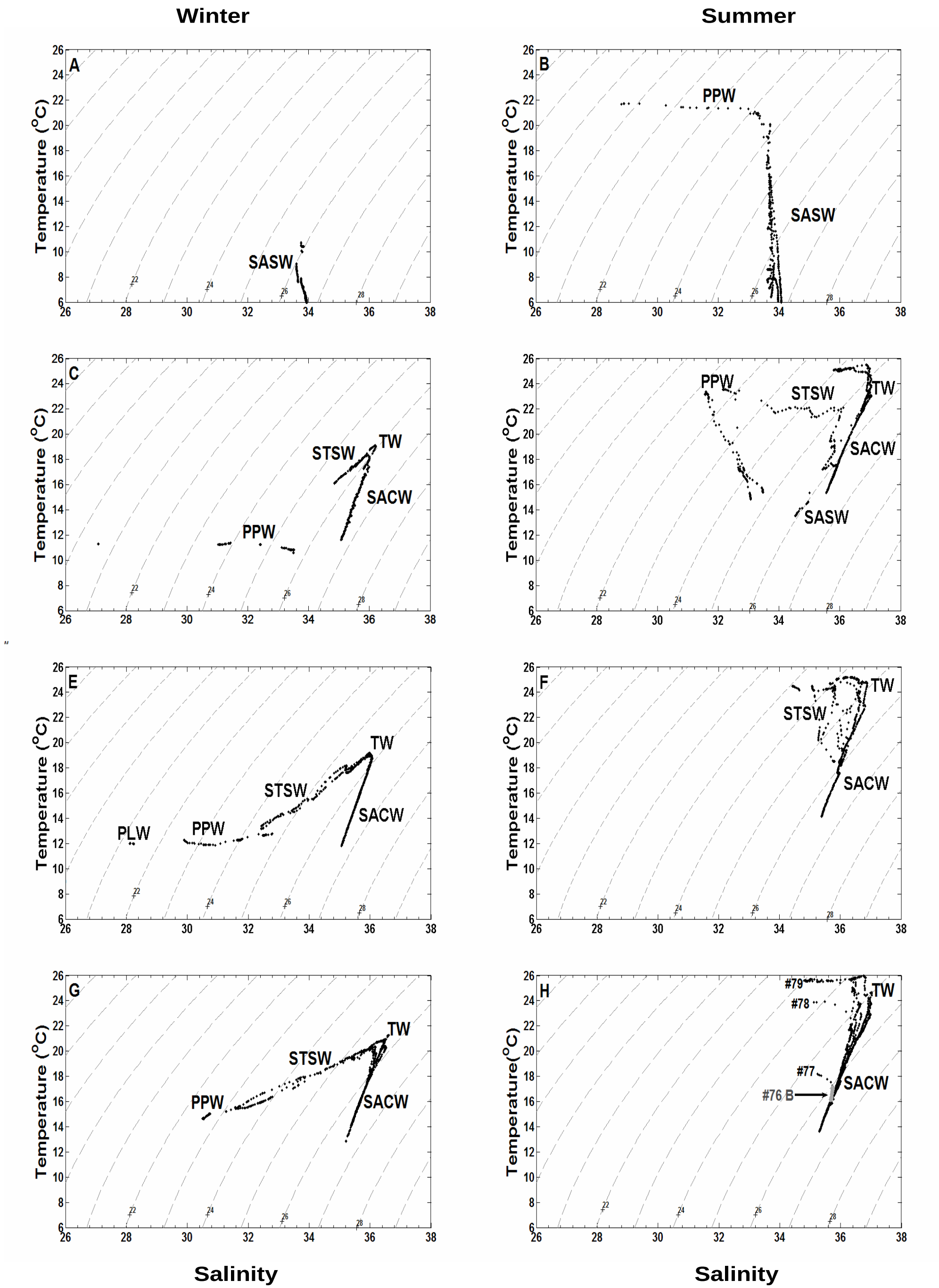

Mar del Plata

Punta Del Diablo

Rio Grande

Cabo de Santa Marta

Moller et al. 2007

The Subtropical Shelf Front: separates subtropical and subantarctic shelf waters

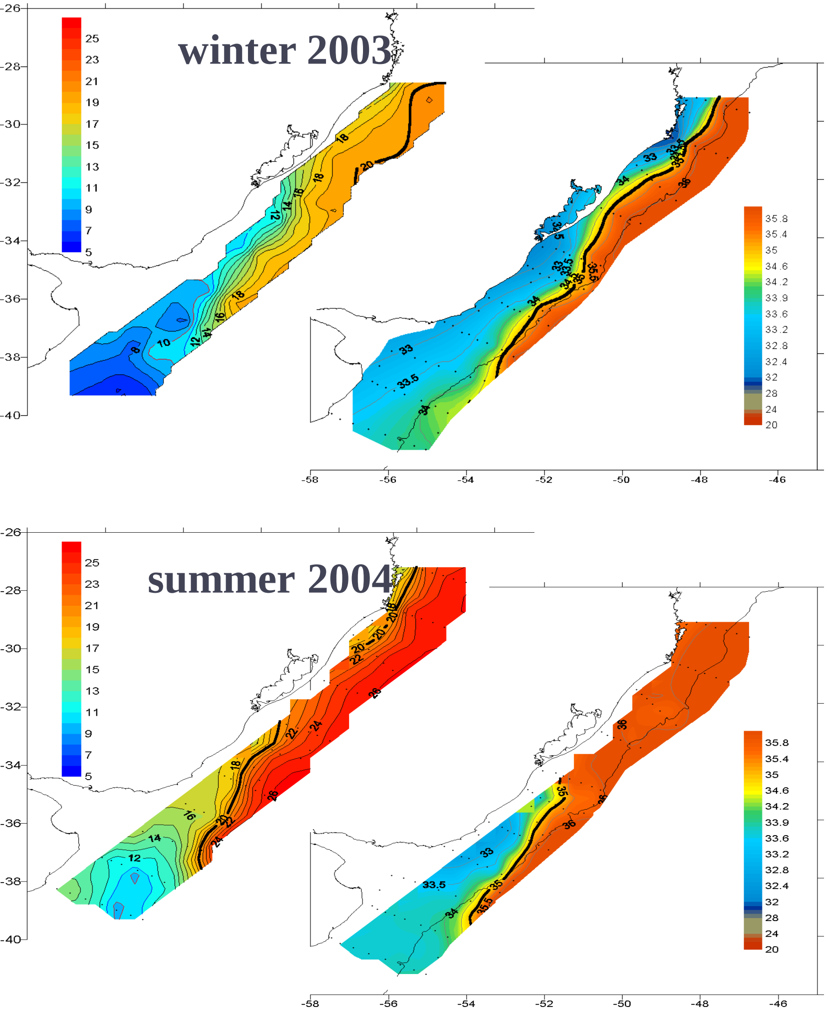

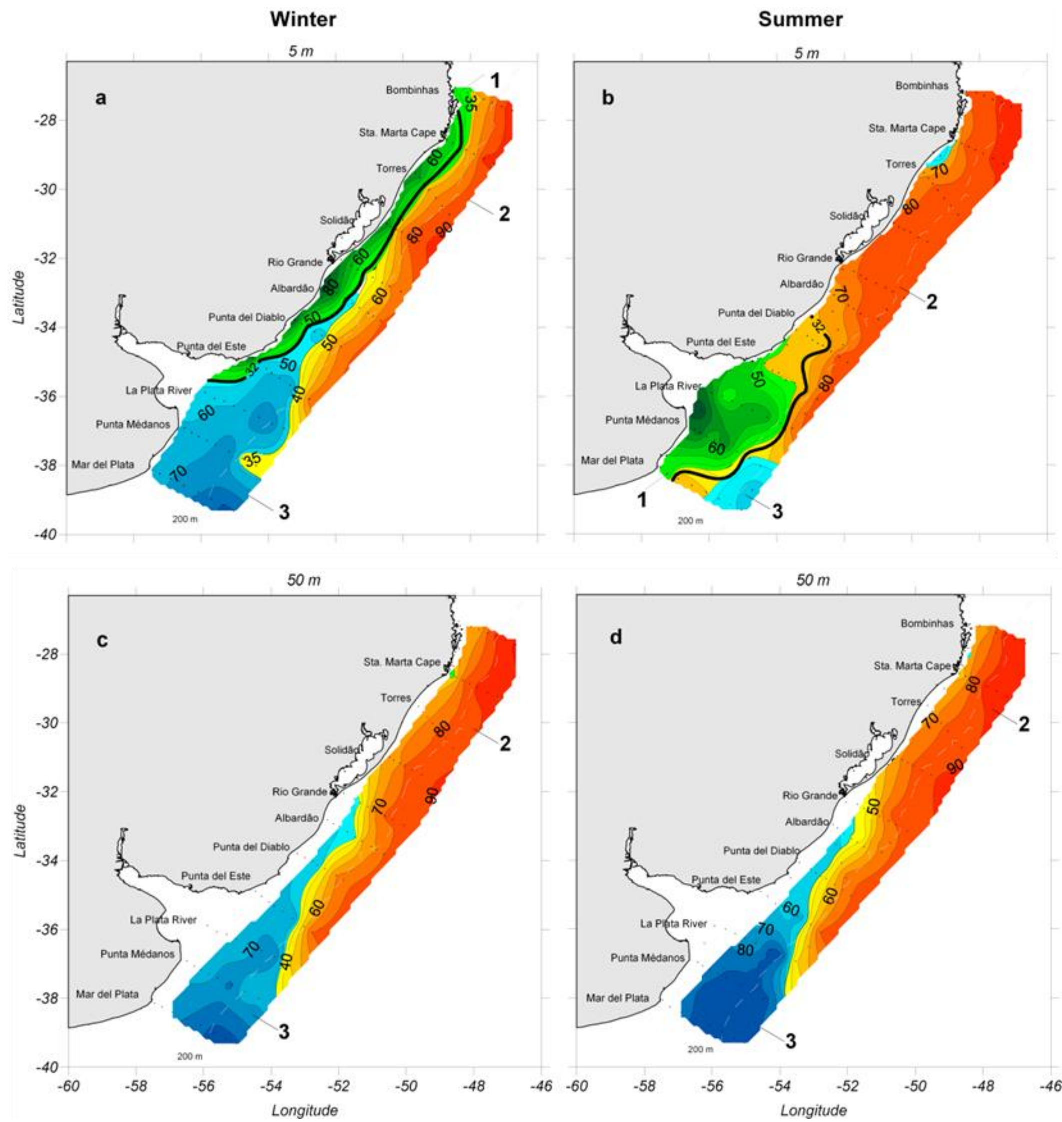

The Subtropical Shelf Front in winter (left) and summer

La Plata - August 2003

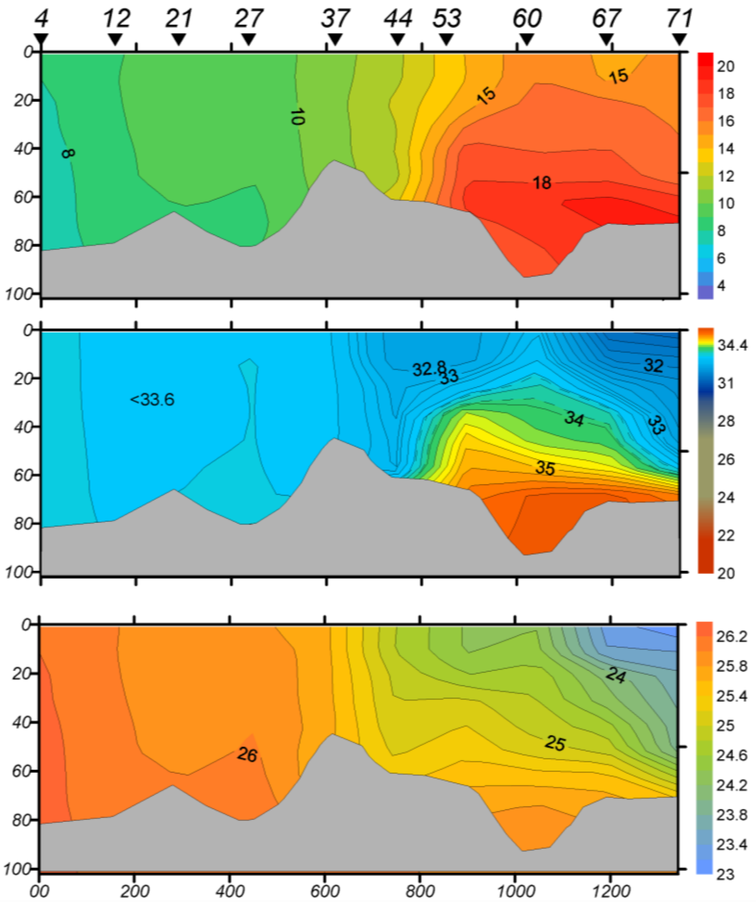

La Plata – February 2004

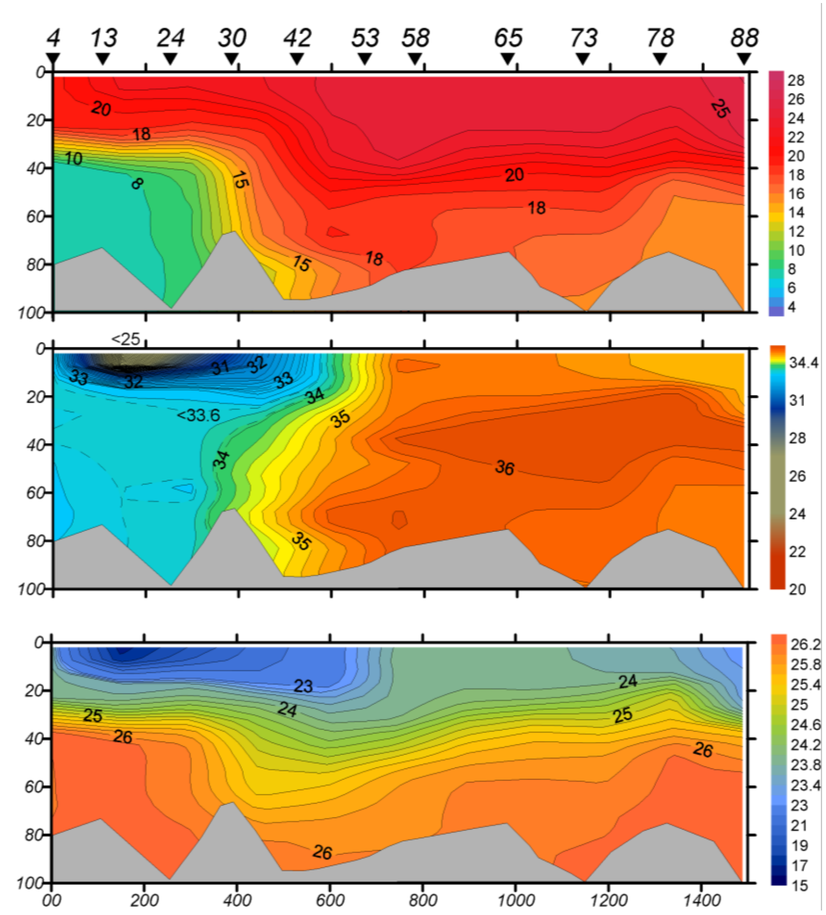

The role of the STSF

We know very little. Normally frontal areas are associated to high biological production. This seems not to be the case. In fact we suspect that it serves as a duct to transport shelf waters to the open ocean.

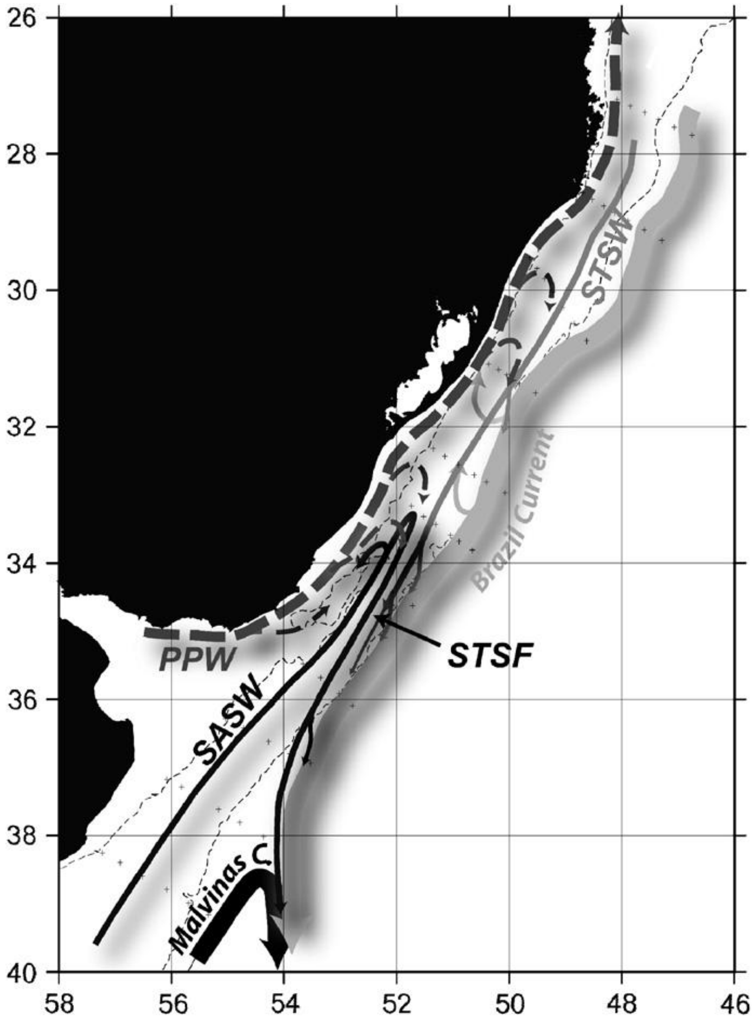

Piola et al. (2008)

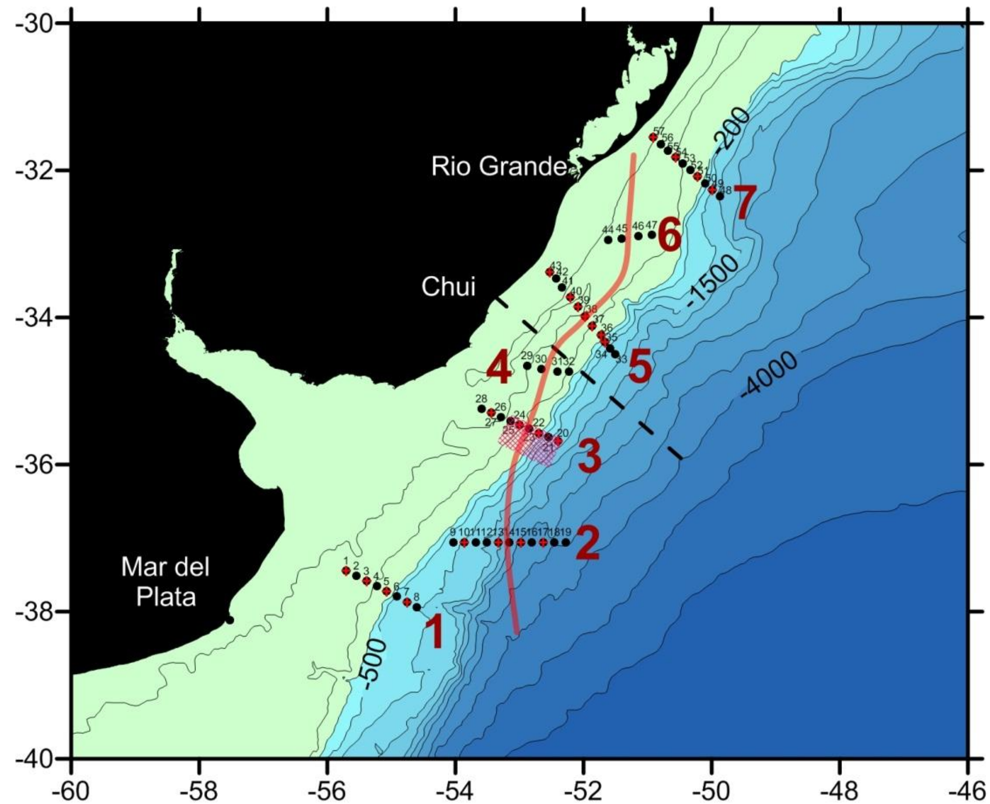

Multidisciplinary cruise focused on the STSF combining ship observations (CTD, DO, Nutrients, plankton, ADCP), 20 – 30 LCDrifters and glider section (3)– october 2012

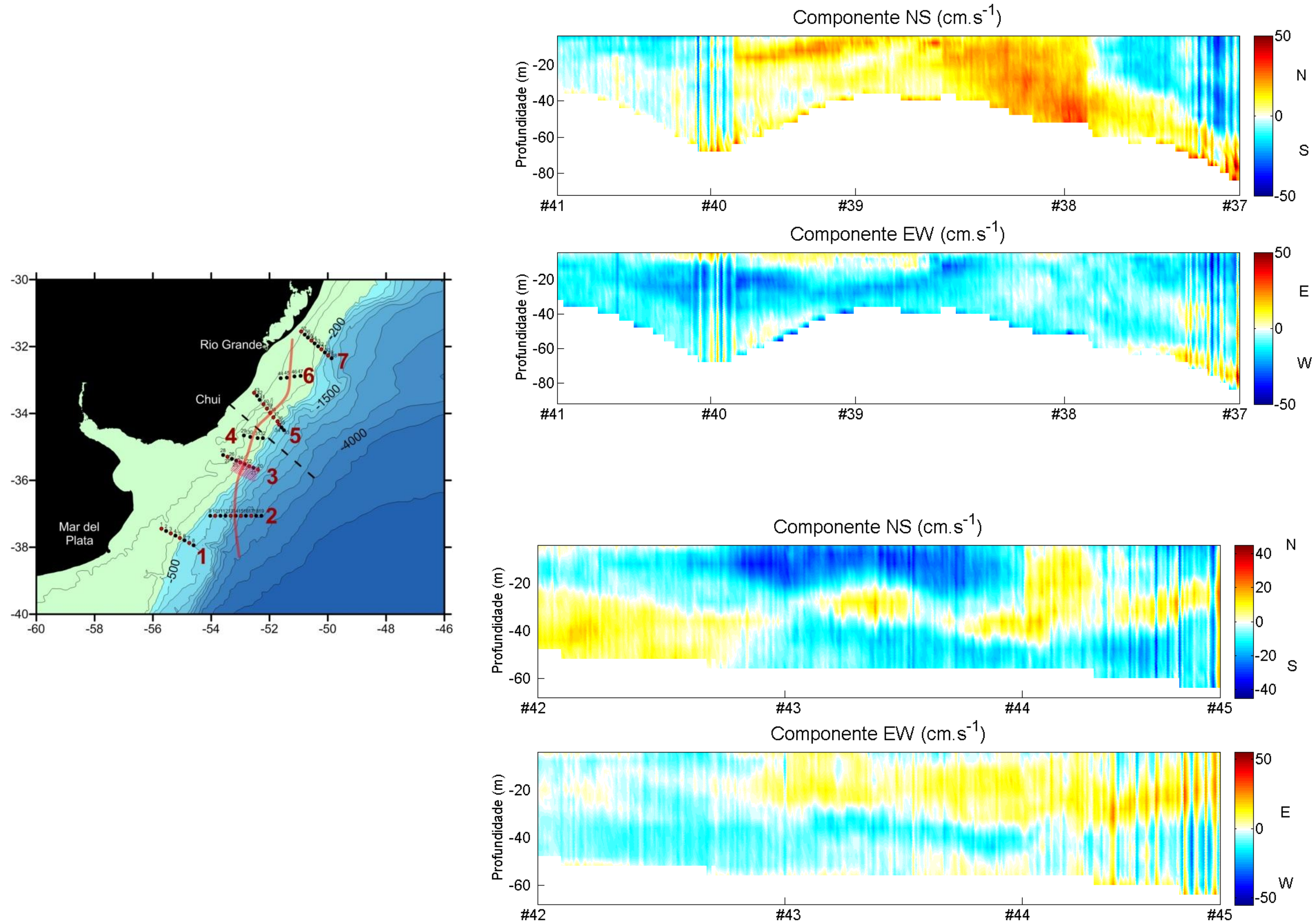

Rio Grande
Chui
Mar del Plata
1
2
3
4
5
6
7
-200
-500
-1500
-4000
-30
-32
-34
-36
-38
-40
-60
-58
-56
-54
-52
-50
-48
-46
Componente NS (cm.s-1)
Componente EW (cm.s-1)
Profundidade (m)
N
S
E
W
50
0
-50
#41
#40
#39
#38
#37
Componente NS (cm.s-1)
Componente EW (cm.s-1)
Profundidade (m)
40
20
-20
-40
#42
#43
#44
#45

Frentes de Marés

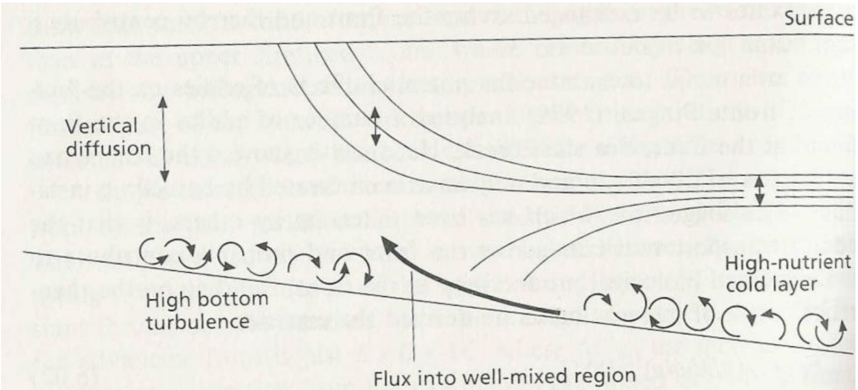

Fig. 6.03 Density section through a tidally-mixed front with vertical arrows indicating the increase in the rate of vertical eddy diffusion from the stratified side to the mixed side. At the bottom higher levels of turbulence help to transport nutrients from the cold, high-nutrient layer into the fully-mixed region.

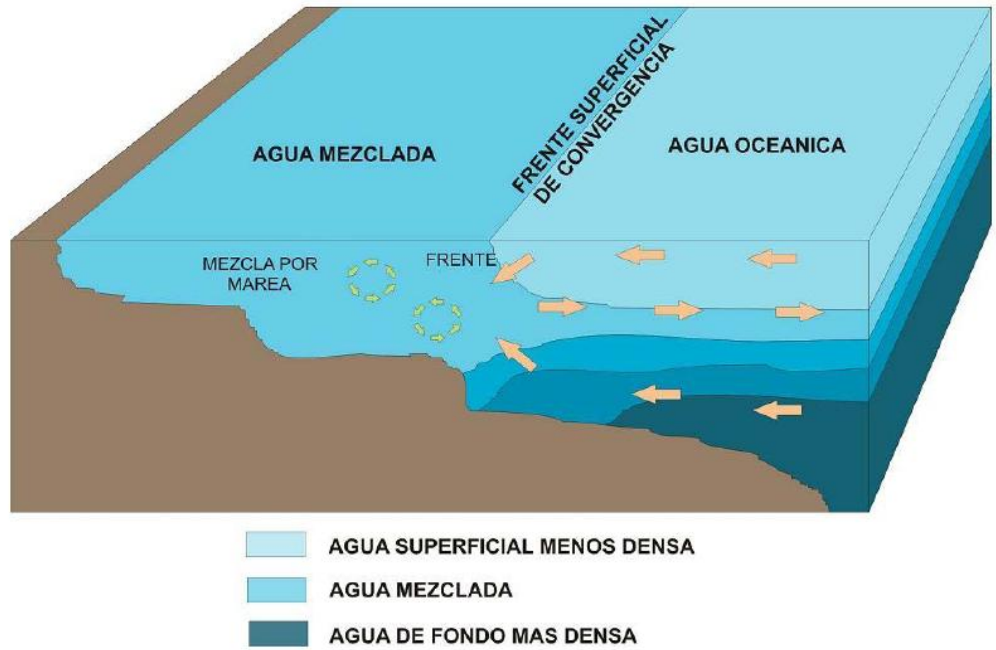

Figura 2-14 Representación esquemática de un frente de marea

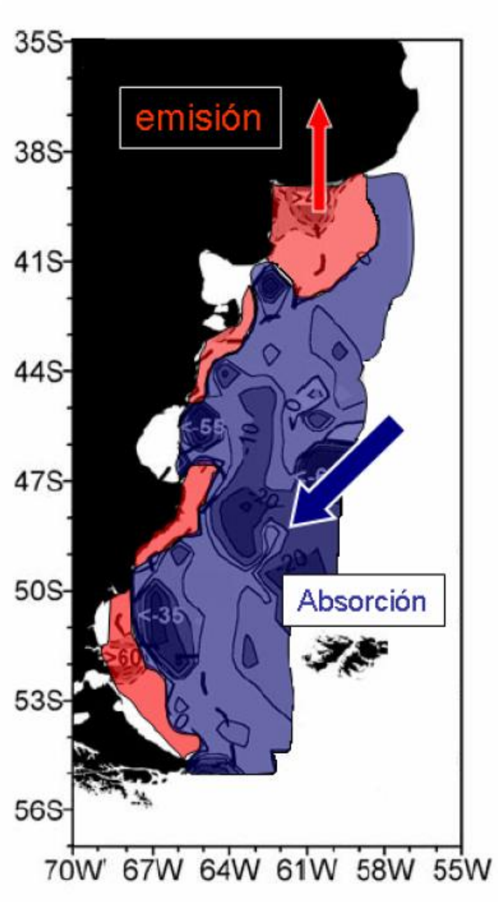

Figura 1-2 Flujos de CO_2

Flujos de CO_2 obtenidos por Bianchi y otros (2005). Estos autores encontraron una clara relación entre los flujos de CO_2 y los frentes de la Plataforma Patagónica, que durante la época cálida separan aguas homogéneas de aguas estratificadas: las zonas costeras mezcladas actúan como fuentes de CO_2 hacia la atmósfera (emisión: zonas sombreadas en rojo), mientras que las aguas estratificadas de la plataforma media y exterior se comportan como sumideros (absorción: zonas sombreadas en azul).

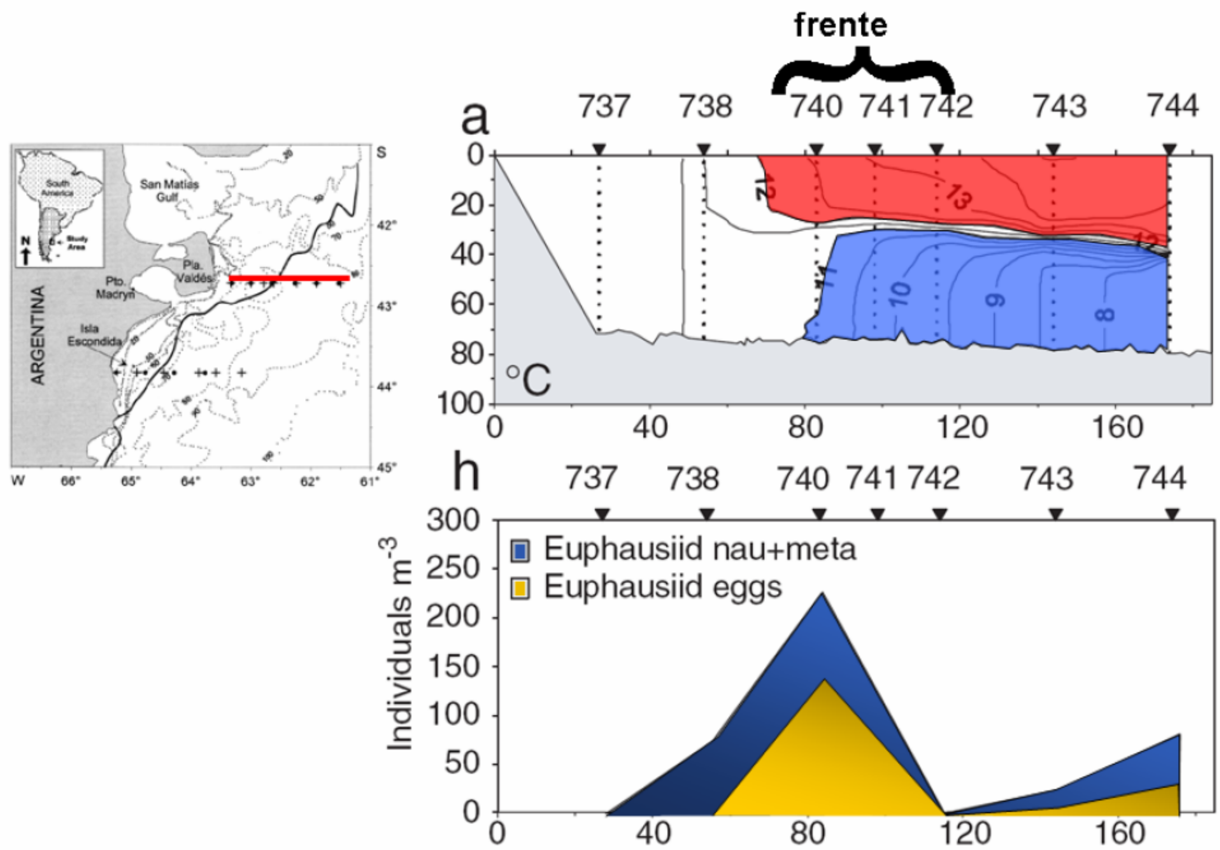

Figura 2-3 Frente Península Valdés

Fig. Adaptada de Sabatini y Martos, 2002 donde se aprecian en los paneles de la derecha la posición del frente térmico en concordancia con la abundancia máxima de huevos de organismos zooplanctónicos.

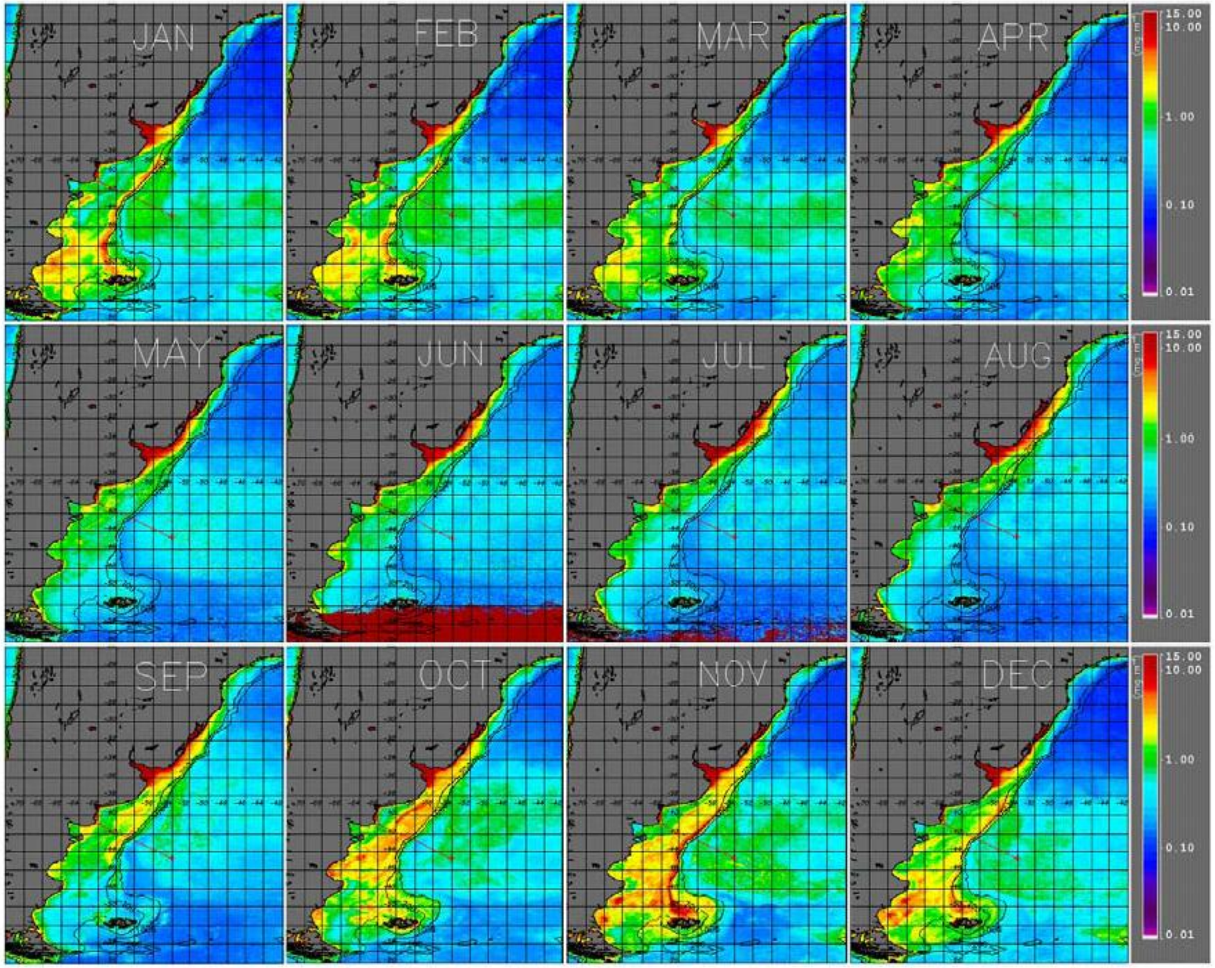

Figura 4-15 Climatologías mensuales de CSAT (1998-2004)

Plumas de rios

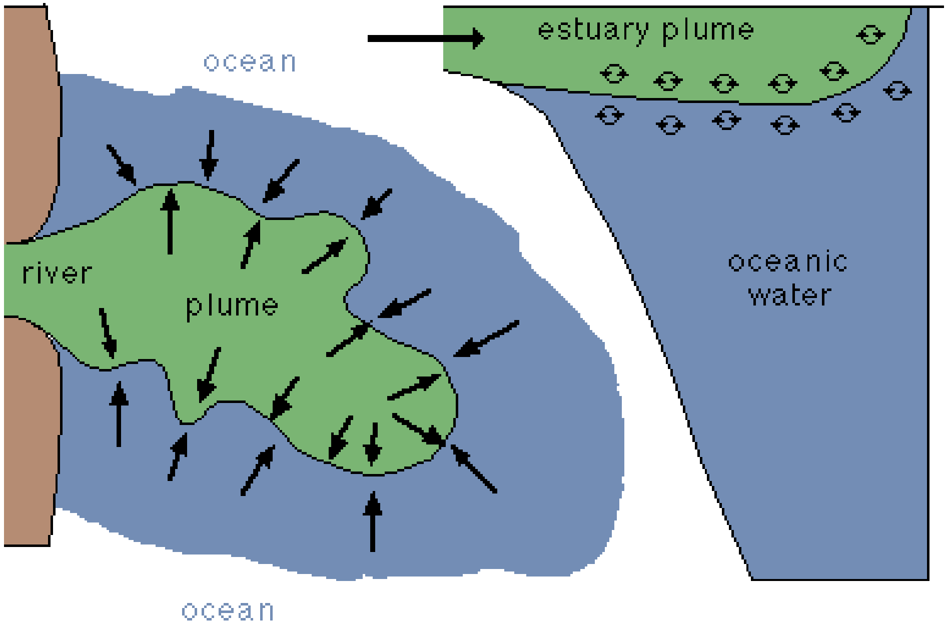

Frentes de Rios (Plumas)

Critérios para classificar frentes de rios

Garvine (1995, 1999)

Número de Kelvin e de Froude

$$K = \frac{L}{r_i}$$

$$r_i = \frac{c_i}{f}$$

$$c_i = \left(\left(\frac{\rho_a - \rho_p}{\rho_a} \right) gH \right)^{0,5}$$

L – largura da pluma

r_i – raio interno de deformação

H – espessura da pluma

1586 R. W. Garvine

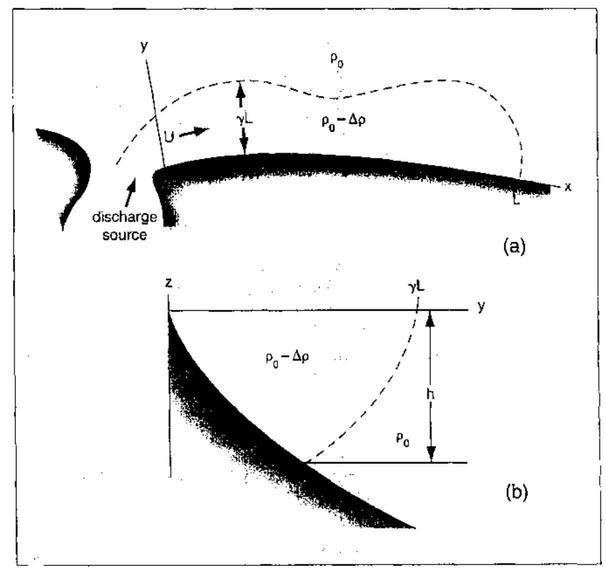

Fig. 1. Defining sketch for buoyant layer scales. (a) x and y are the alongshore and across-shore co-ordinates. Dashed line denotes a typical bounding isopycnal contour for the buoyant layer whose typical density is $\rho_0 - \Delta\rho$. Coastal water has typical density ρ_0. U is the typical alongshore buoyant water velocity, L the alongshore length scale, and γL the across-shore-length scale. (b) A typical across-shore vertical section with vertical coordinate z. Dashed line shows typical bounding isopycnal for the buoyant layer of typical depth h.

Número de Froude – F

Representa o equilíbrio entre inércia e a gravidade (flutuabilidade).

$$F = \frac{V_r}{c_i}$$

V_r – velocidade do rio

Q_i – descarga (Q) do rio por unidade de largura (B)

Qi=Q/B

$$V_r = \left(g' Q_i\right)^{1/3}$$

F = 1, critical flow,
F > 1, supercritical flow (fast rapid flow),
F < 1, subcritical flow (slow / tranquil flow)

- Quando K<<1 a largura da pluma é muito menor do que o raio interno de deformação e temos uma pluma de pequena escala (a menos que seja locada no equador). Assim, o termo de Coriolis não é importante na equação do movimento e o gradiente de pressão é equilibrado por termos advectivos (inerciais). São normalmente fluxos rápidos com pouca não linearidade. Como a descarga é alta, o número de Froude é igual ou maior que 1. A razão comprimento/largura é 1.

- Quando K>>1 o termo de Coriolis se torna importante e a pluma está em equilíbrio geostrófico. A razão comprimento/largura é maior que 1. As velocidades são baixas e o número de Froude é menor do que 1.

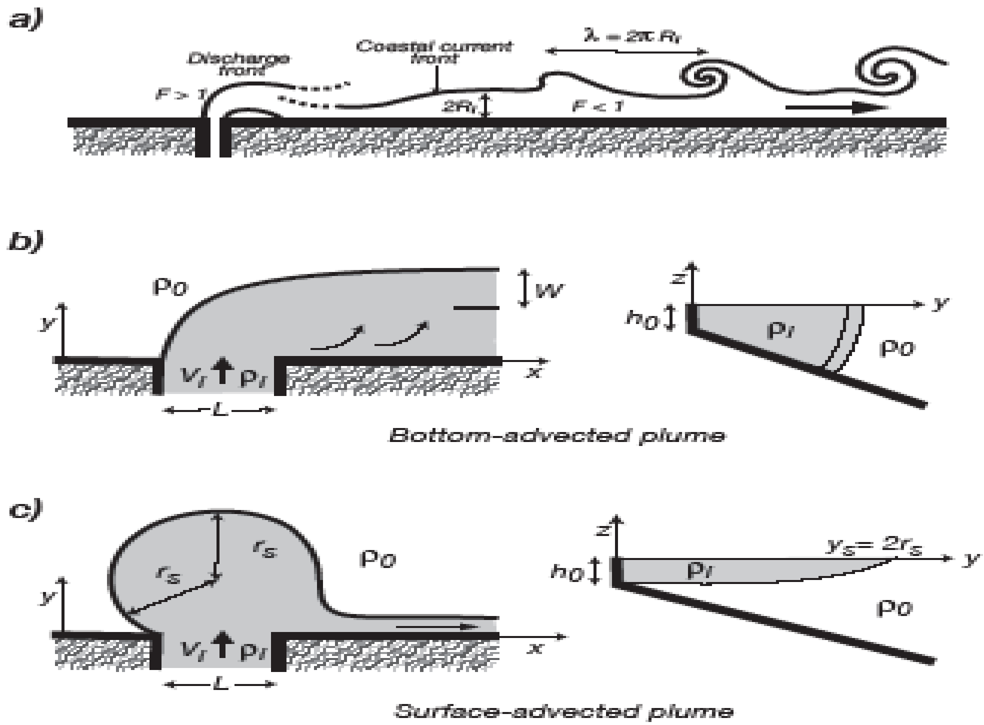

Figure 10.2. Schematics of a buoyant plume in the coastal ocean. a) Large coastal plume turns anticyclonically and reattaches to the coast downstream to form a narrow buoyancy driven current upon which meanders and instabilities develop (adapted from Hill, 1998). Froude number (*F*) indicates that the dynamics is supercritical (*F*>1) in the bulge, and subcritical (*F*<1) in the far field; the Internal Rossby number (R_I) scales the buoyant current. b,c) Bottom-advected and surface-advected plume (after Yankovsky and Chapman, 1997); ρ_i,ρ_o density of inflow and ambient flow, h_0 and L are the depth and width at the estuary, W is the frontal region width, r_s the plume's bulge radius and y_s the plume's location offshore.

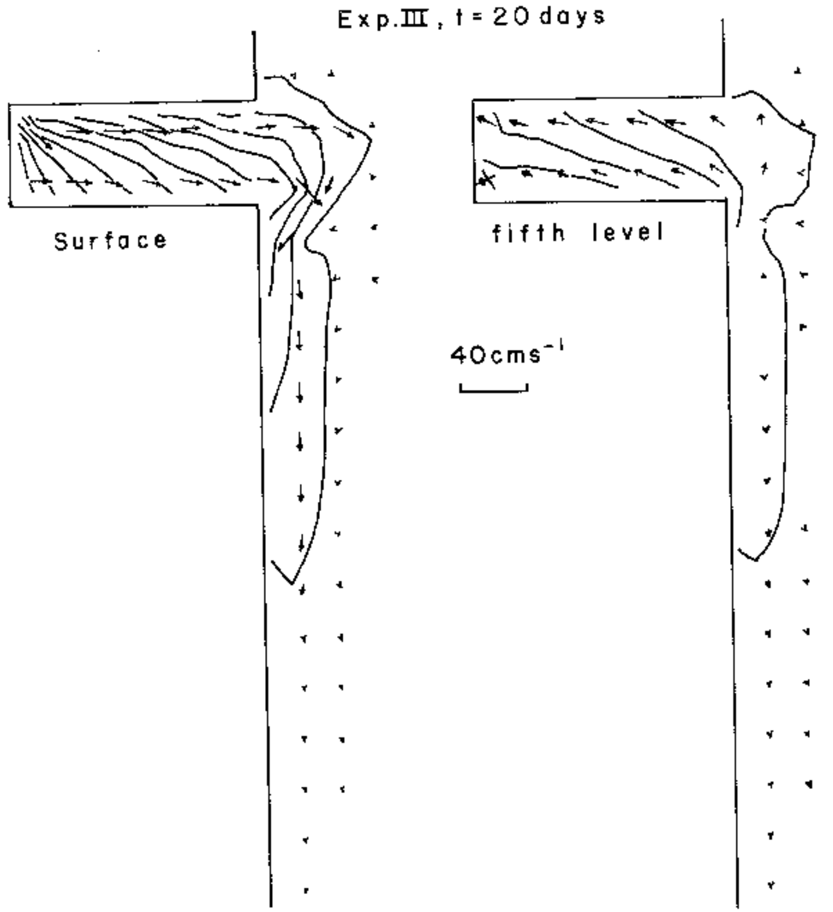

FIG. 16. As in Fig. 4 except for the third experiment at t = 20 days, and the salinity contour is 0.8 ppt. A sloping shelf reduces the seaward excursion of the bulge.

- Ajuste geostrófico
- Efeito do vento
  - A)favorável à ressuregência
  - B) contrário à ressurgência

Efeito da Maré

Efeito da morfologia ângulo limite de 66º com a costa – acima disto a pluma não “cola” na costa (Garvine, 1982)

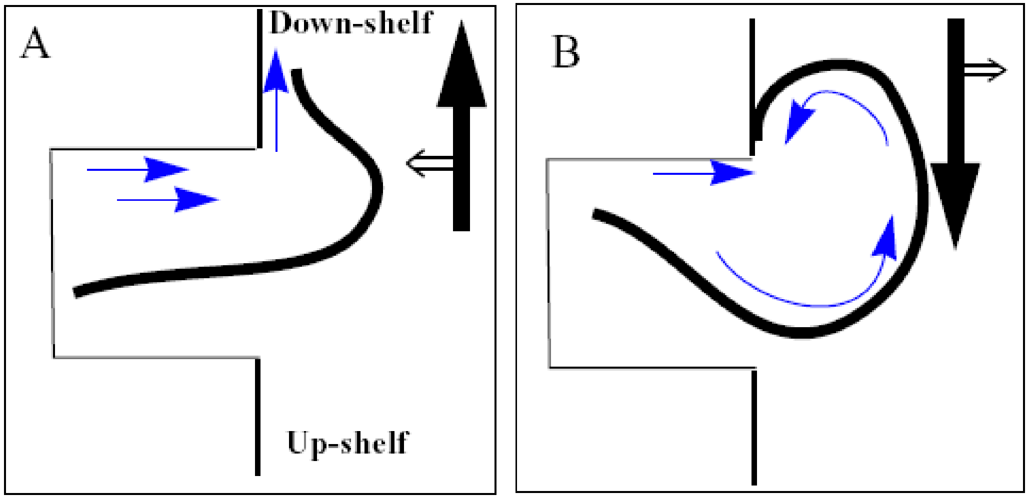

FIGURE 2. Sketch of buoyant discharge under downwelling (A) and upwelling (B) wind conditions on the shelf (*southern hemisphere*). The thick (filled) and thin (open) arrows indicate wind direction and associated surface Ekman flux, respectively. Blue arrows represent circulation and thick lines indicate the buoyant plume.

Garvine, 2000

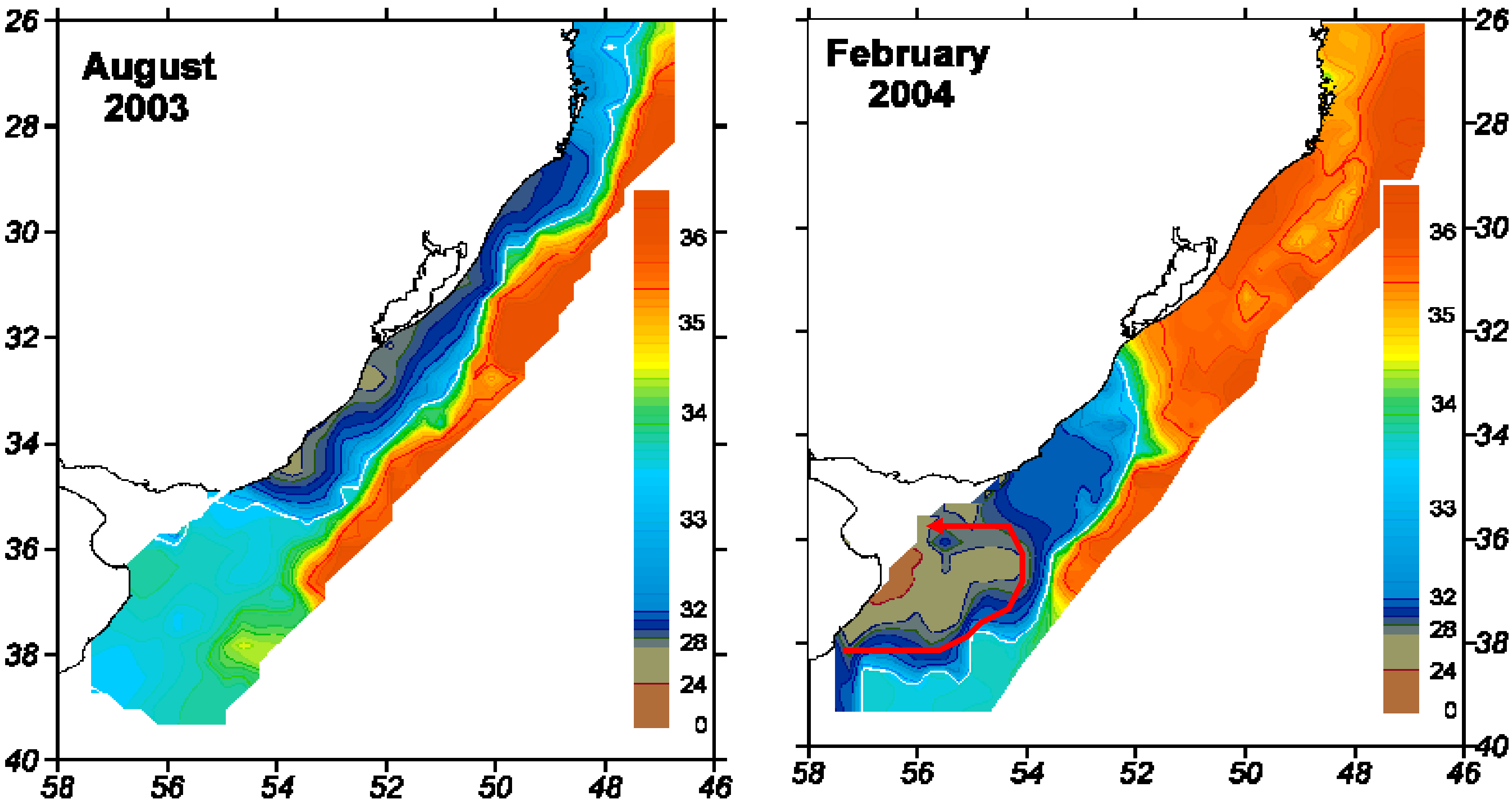

August
2003
February
2004
26
28
30
32
34
36
38
40
58
56
54
52
50
48
46
36
35
34
33
32
28
24
0

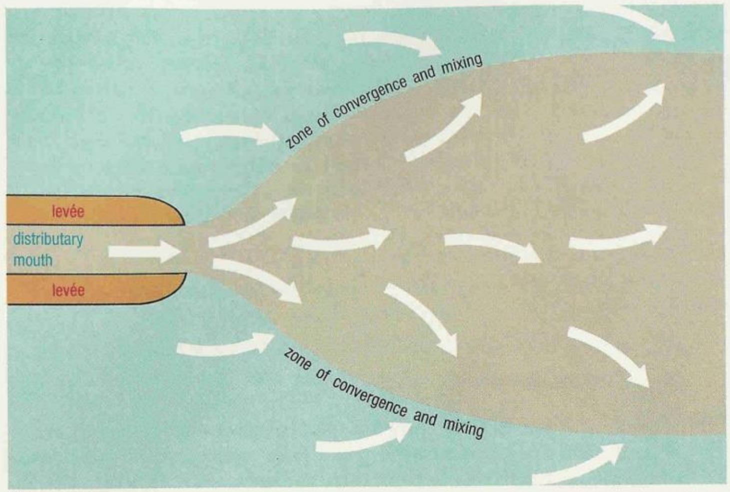
zone of convergence and mixing
levée
distributary
mouth
levée
zone of convergence and mixing

(a)

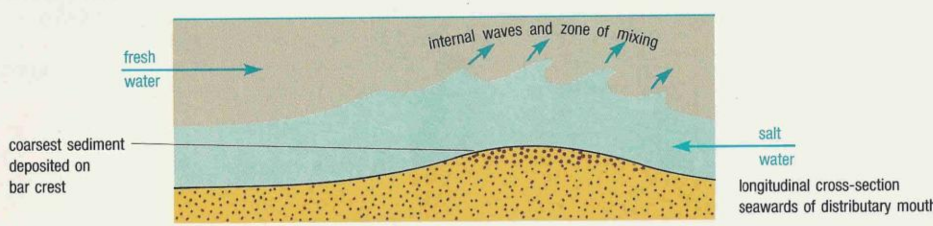
internal waves and zone of mixing
fresh
water
coarsest sediment
deposited on
bar crest
salt
water
longitudinal cross-section
seawards of distributary mouth

(b)

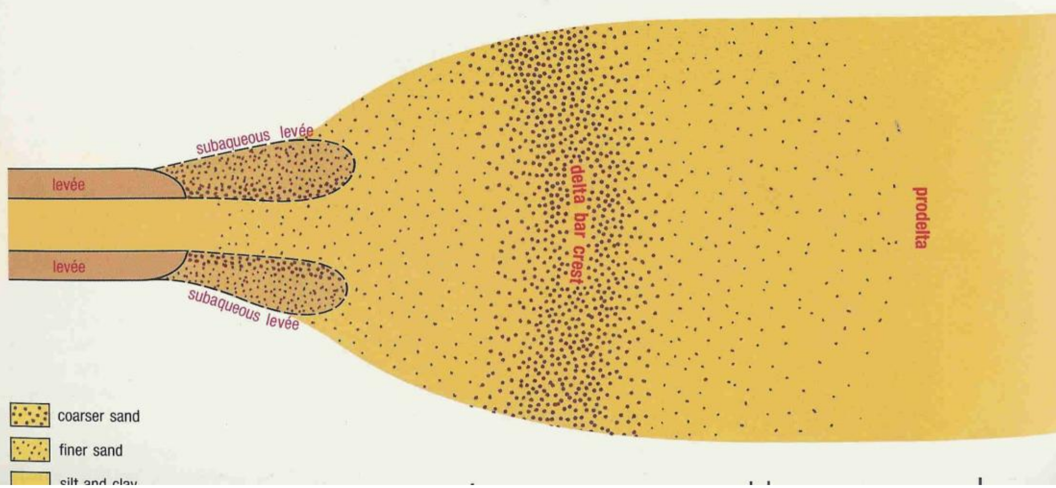
subaqueous levée
levée
levée
subaqueous levée
delta bar crest
prodelta
coarser sand
finer sand

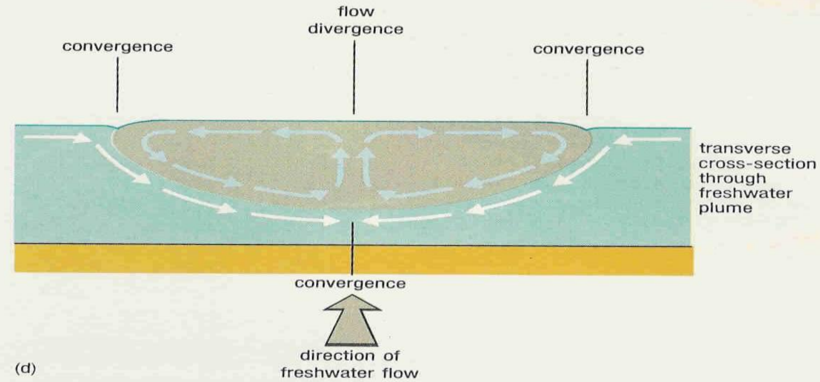

(d)

Turbulent mixing

When the speed of the fluvial discharge is high, then the outflow is turbulent; vigorous mixing occurs with the seawater and so density stratification cannot occur. In the case of the River Amazon, the river outflow is so powerful that it literally forces the salt water back, seawards of the delta bar crest. If the high speed river water is discharged into moderately deep water, then turbulent mixing occurs in three dimensions and the plume can expand both vertically and laterally. However, because of the vertical expansion, the amount of lateral expansion is reduced and the angle of spreading is relatively small (Figure 7.7(a)). As the water is deep, mixing does not occur right down to the bed which is overlain by a layer of unmixed seawater (Figure 7.7(b)).

Would you expect any residual flow (Section 6.2.1) in this seawater layer?

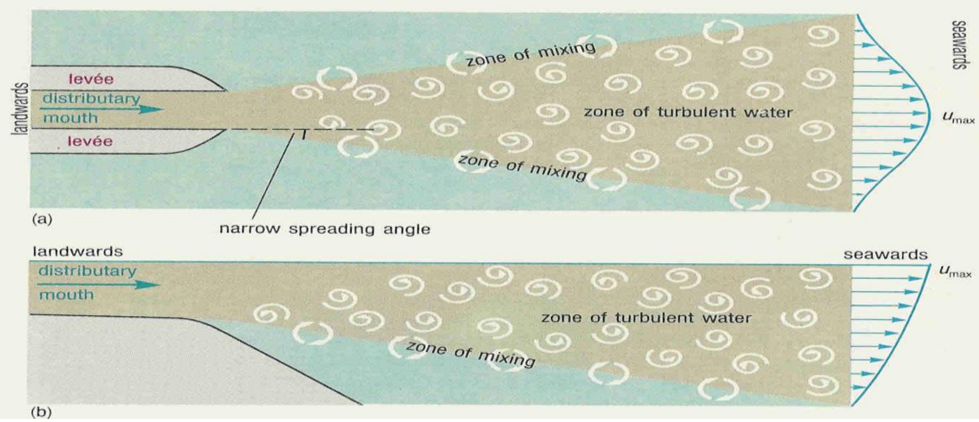

Figure 7.8 The patterns of spreading, turbulent mixing and flow deceleration which occur when the river discharge is high, but into shallow water. The length of the blue arrows is proportional to the freshwater flow velocity and u_{max} is the maximum flow velocity.

(a) Schematic plan view of the distributary mouth to show the wide spreading angle and the freshwater flow velocities at the seawards edge of the plume.

(b) Schematic cross-section of (a) to show turbulent mixing occurring down to the bed. The two velocity profiles show the rapid deceleration of the freshwater flow.

(c) As the freshwater flow decelerates, deposition occurs rapidly, blocking the distributary mouth. The turbulent discharge therefore bifurcates isolating a sediment bar between two new channels and their associated subaqueous levées.

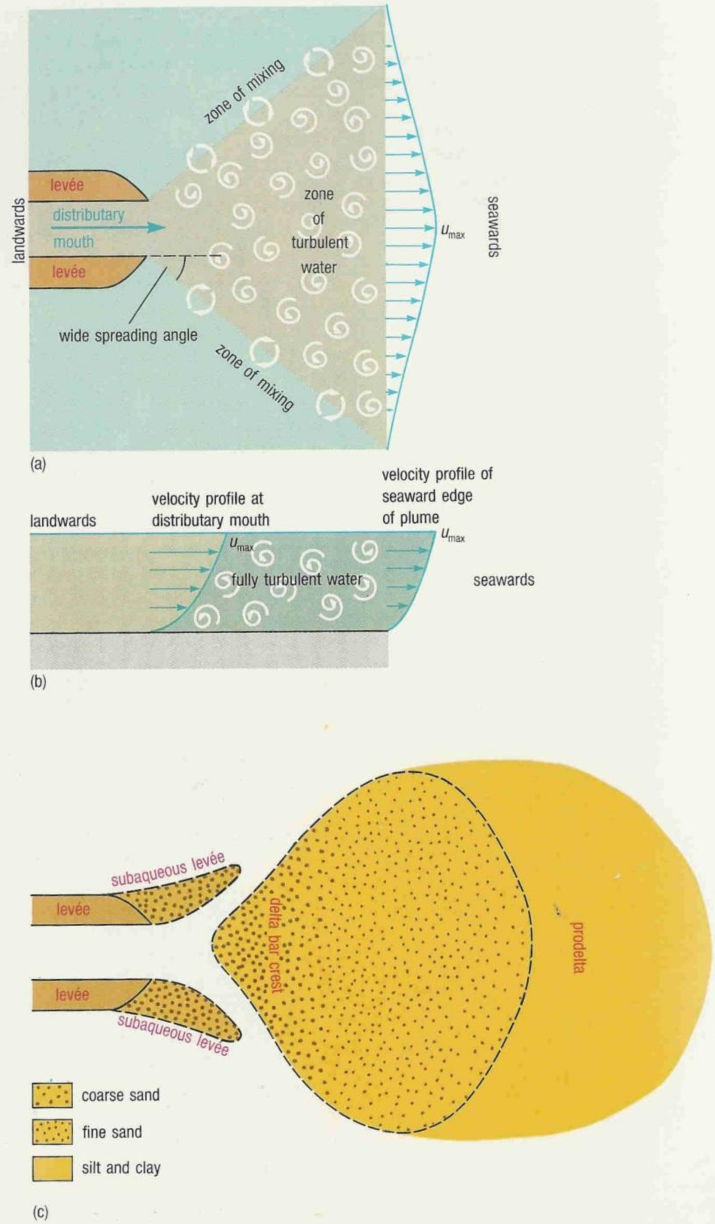

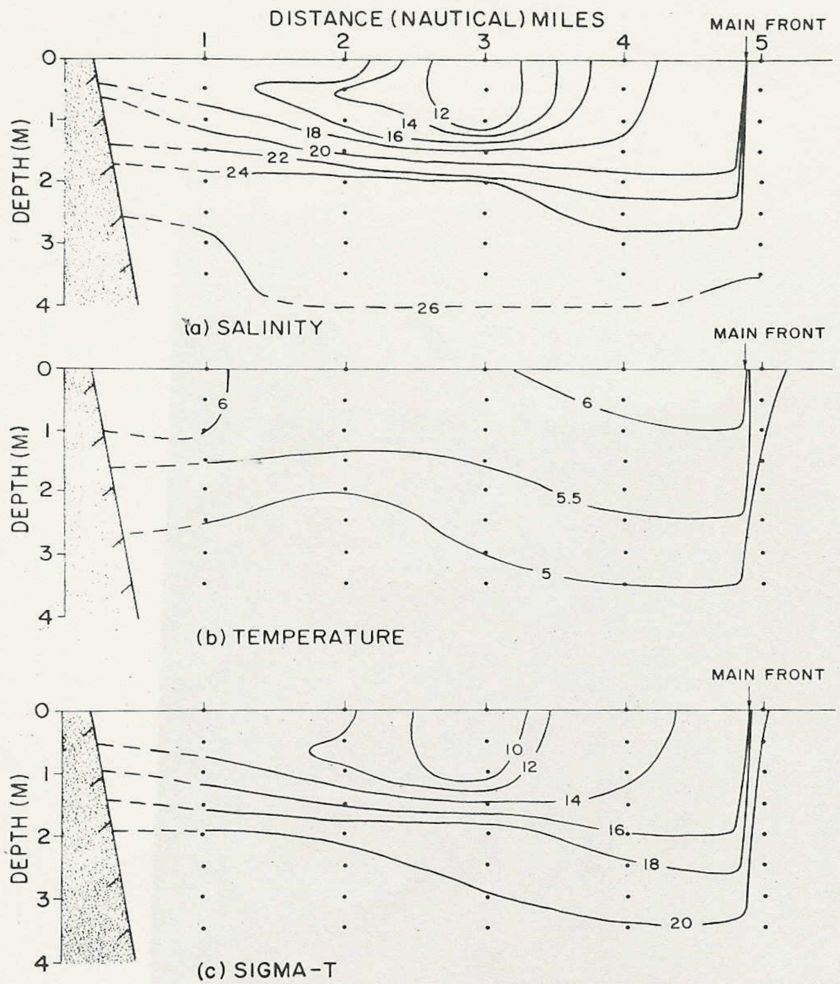

Fig. 1. Hydrographic section of the Connecticut River plume normal to the plume axis, April 13, 1973. (*a*) Salinity (per mil). (*b*) Temperature (degrees Celsius). (*c*) Density (sigma-t). Data are from *Garvine* [1974].

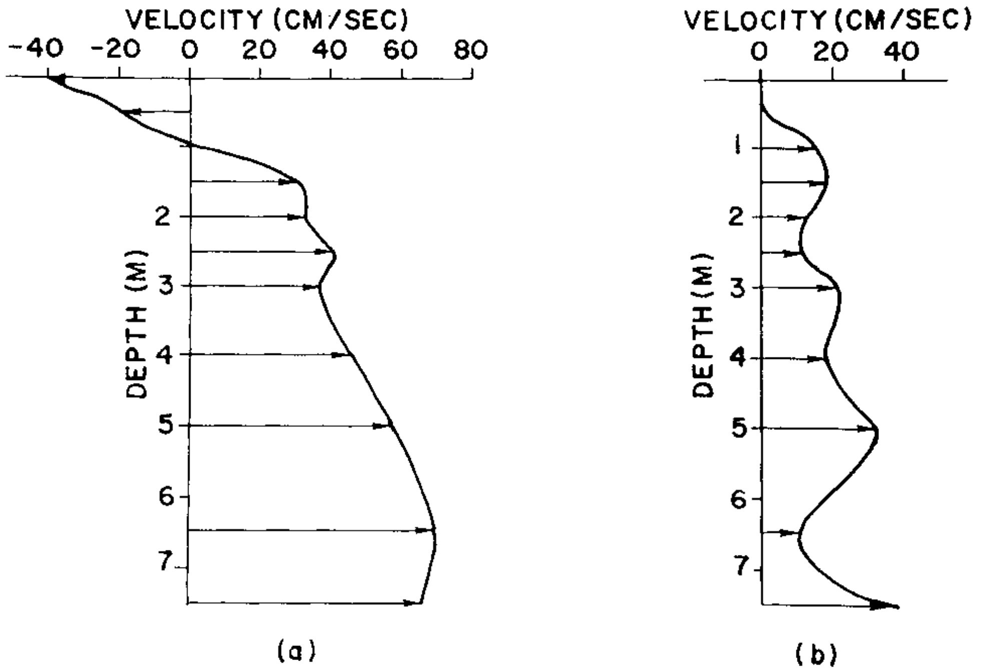

Fig. 5. Horizontal velocity versus depth on March 16, 1973, taken 30 m from the color front on the brackish water side. The arrows correspond to the depths of measurement. (*a*) Velocity component normal to the front (positive toward freshwater). (*b*) Velocity component parallel to the front (positive away from the river mouth).

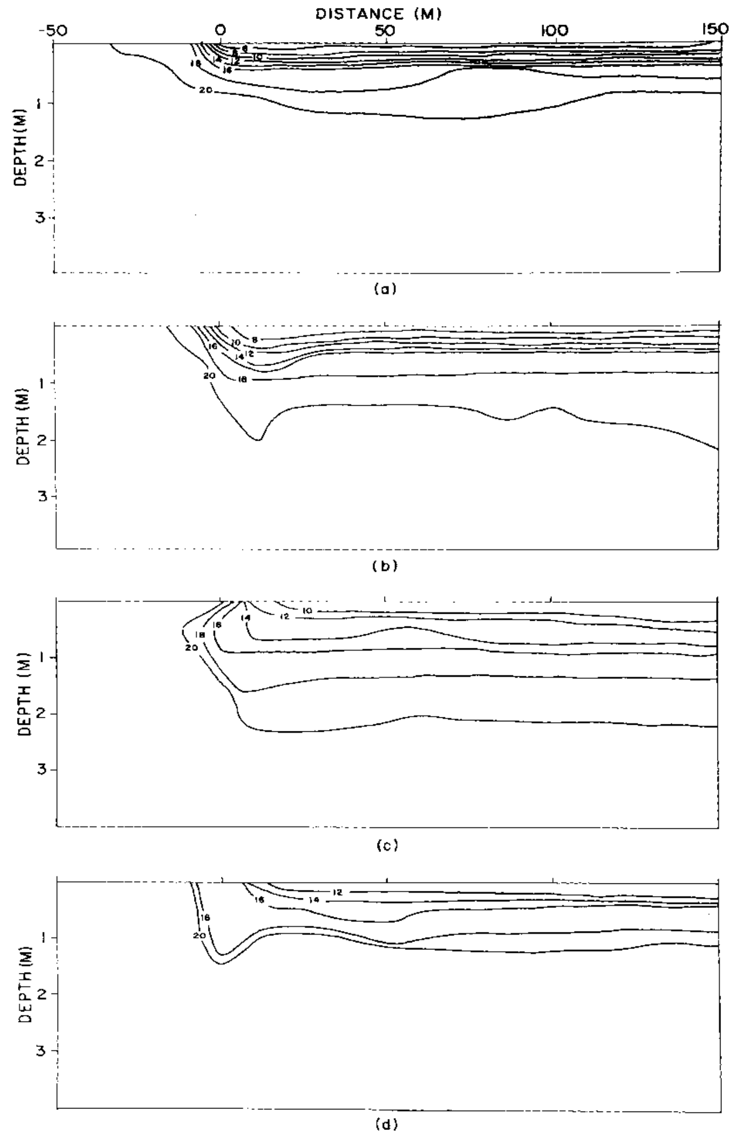

Fig. 10. Density (sigma-t) sections normal to the color front on May 14, 1973. Measurements were made in four time intervals (EDT): (*a*) 1400-1430, (*b*) 1430-1512, (*c*) 1512-1543, and (*d*) 1543-1610.

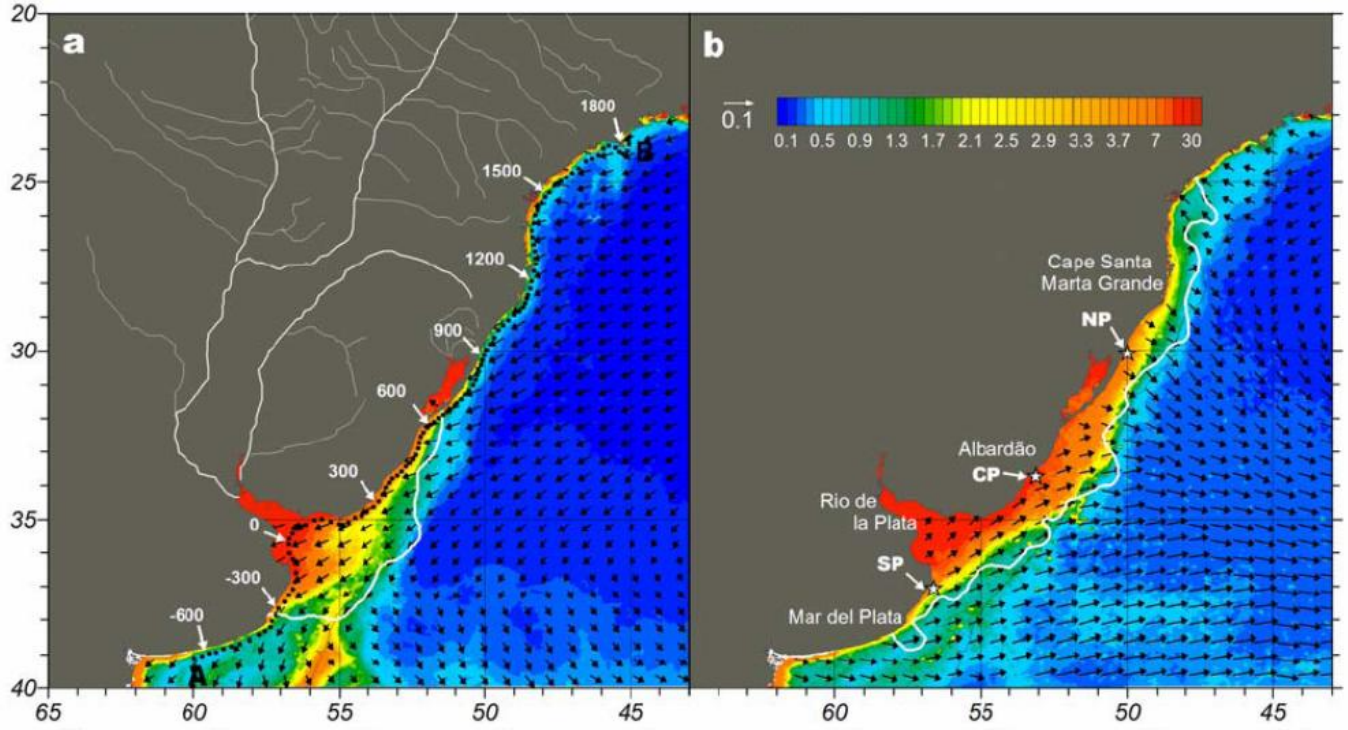

Figura 5-6 Distribuciones climatológicas de CSAT y QuickScat

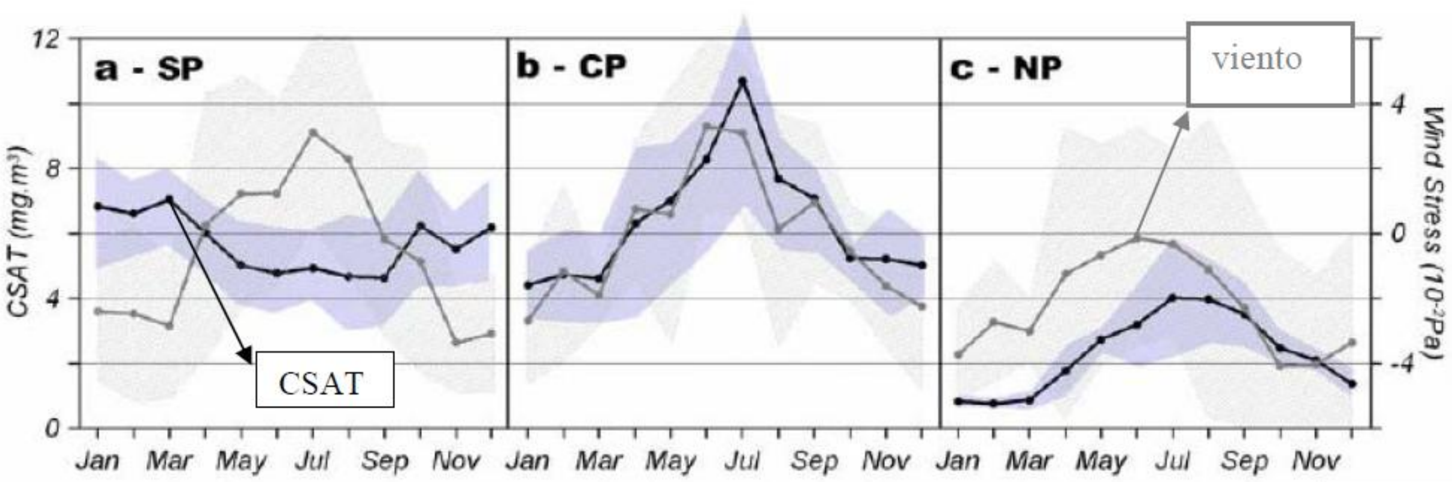

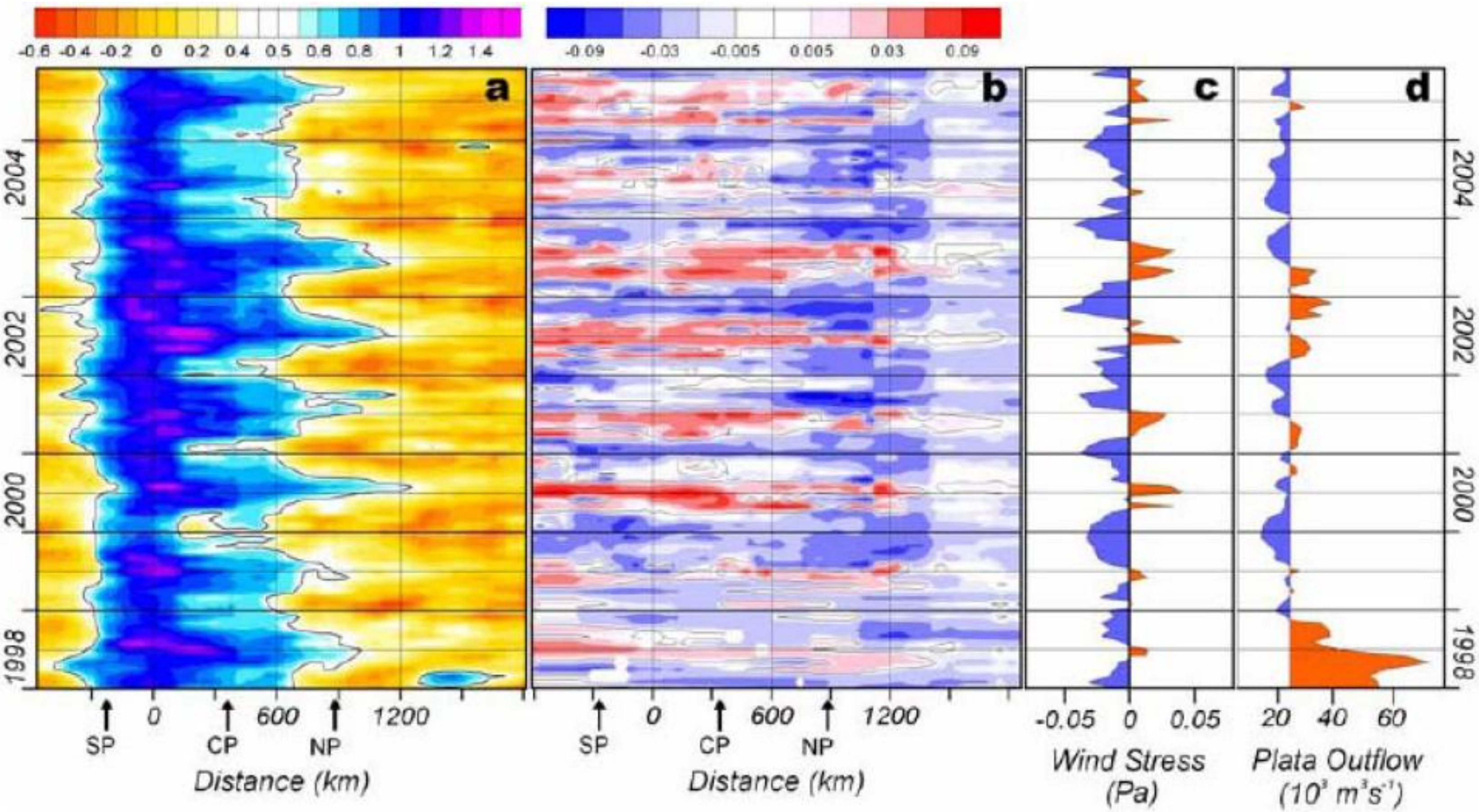

Figura 5-21 Hovmoller de valores medios mensuales de log(CSAT, mg m^{-3})

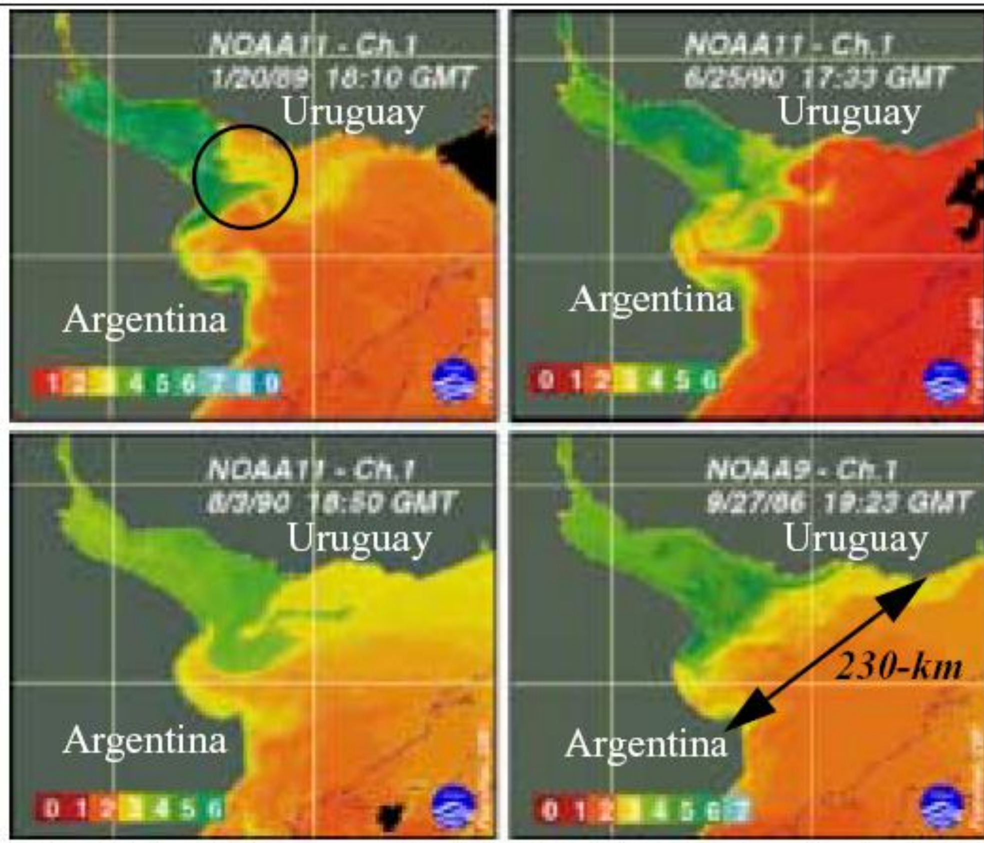

FIGURE 4. Visible channel 1 of NOAA-AVHRR indicating turbidity fronts in the Rio de la Plata estuary/shelf system (see Framiñan and Brown, 1996). See Fig. 1 (p. C-2) for location and bottom topography (modified from Framiñan, per. comm.). The circle in the top left panel indicates the turbidity maximum zone where largest tidal currents occur.

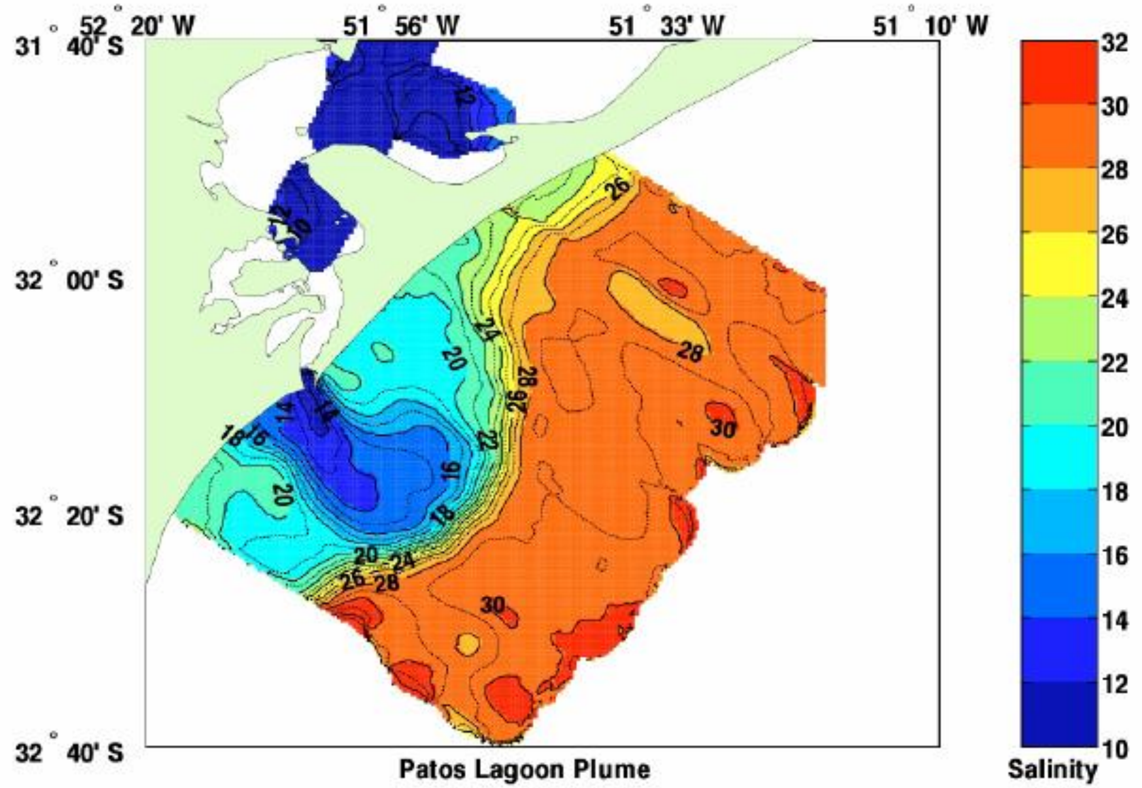

52° 20' W
51° 56' W
51° 33' W
51° 10' W
31° 40' S
32° 00' S
32° 20' S
32° 40' S
Patos Lagoon Plume
Salinity
32
30
28
26
24
22
20
18
16
14
12
10

a)

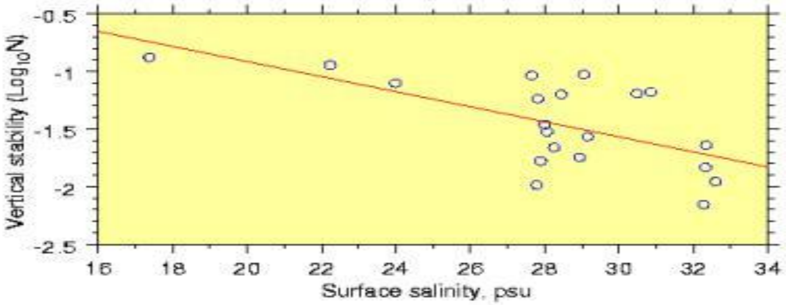

Vertical stability (Log10N)
-0.5
-1
-1.5
-2
-2.5
16
18
20
22
24
26
28
30
32
34
Surface salinity, psu

b)

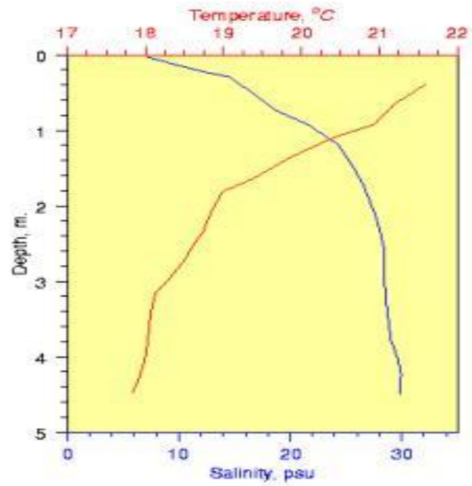

Temperature, °C
17
18
19
20
21
22
Depth, m.
0
1
2
3
4
5
0
10
20
30
Salinity, psu

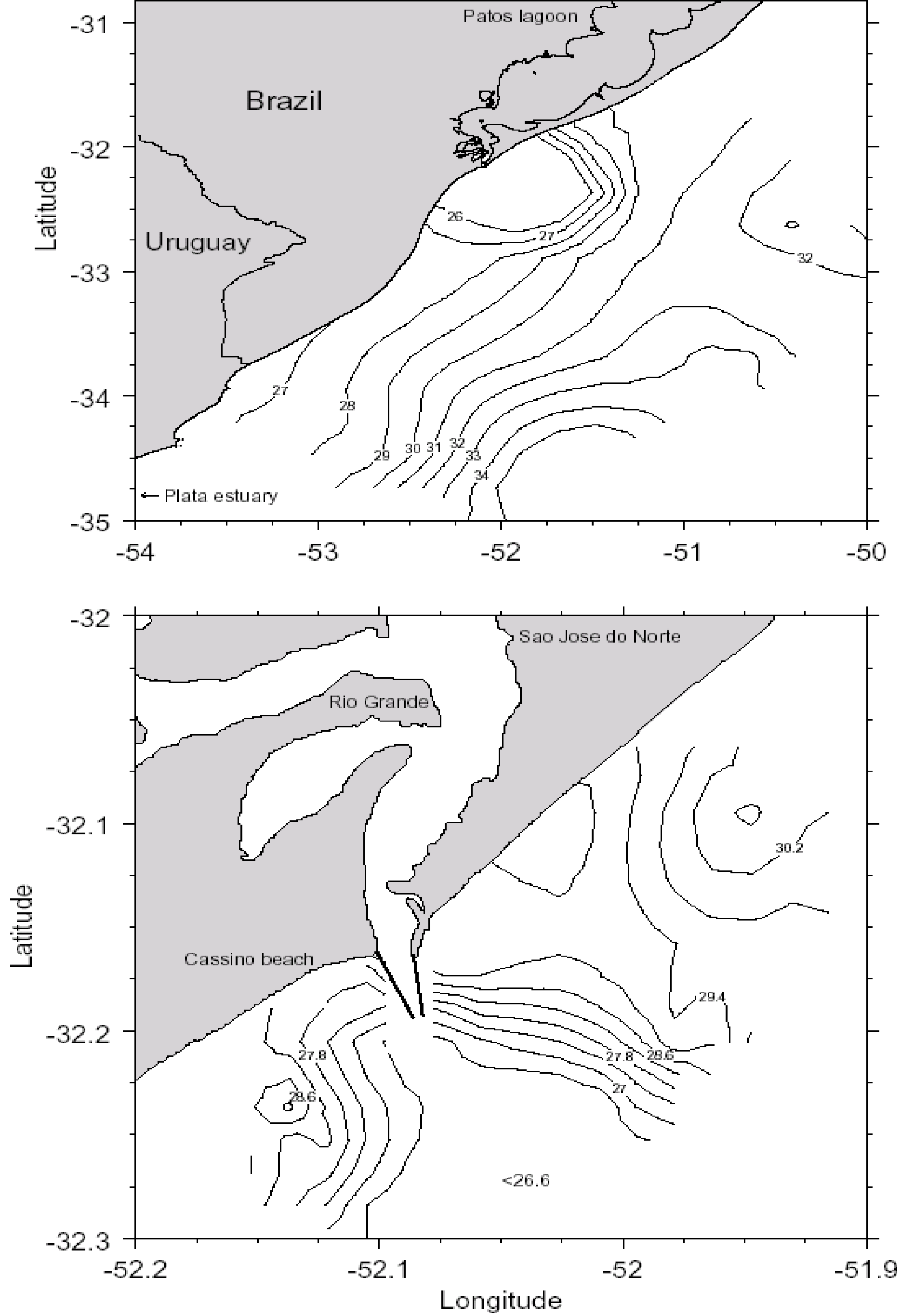
Patos lagoon
Brazil
Uruguay
Plata estuary
Latitude
-31
-32
-33
-34
-35
-54
-53
-52
-51
-50
26
27
28
29
30
31
32
33
34
Sao Jose do Norte
Rio Grande
Cassino beach
30.2
29.4
27.8
28.6
<26.6
-32.1
-32.2
-32.3
-52.2
-52.1
-51.9
Longitude

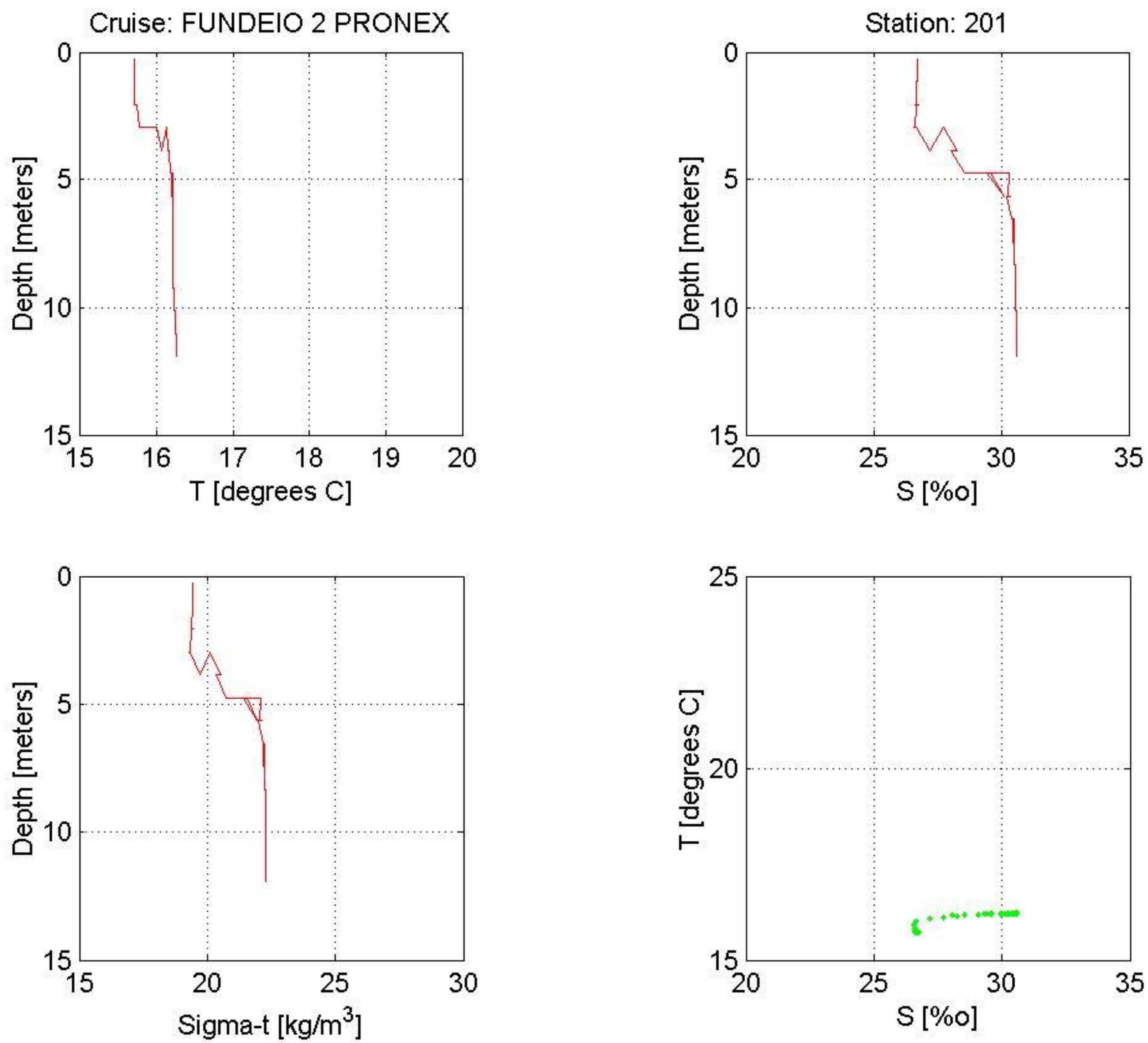

Cruise: FUNDEIO 2 PRONEX
Station: 201
Depth [meters]
T [degrees C]
S [%o]
Sigma-t [kg/m3]
T [degrees C]
S [%o]
0
5
10
15
15
16
17
18
19
20
20
25
30
35
30

Interaciones plataforma -océano

Por ser una área compleja, en general, necesitamos:

a) más estudios multidisciplinares, integrados y de resolución fina;

b) series temporales

c) estudios que involucren las interaccion plataforma-océano abierto;

d) conocer el rol de estas aguas en los procesos de absorción/liberación de CO2

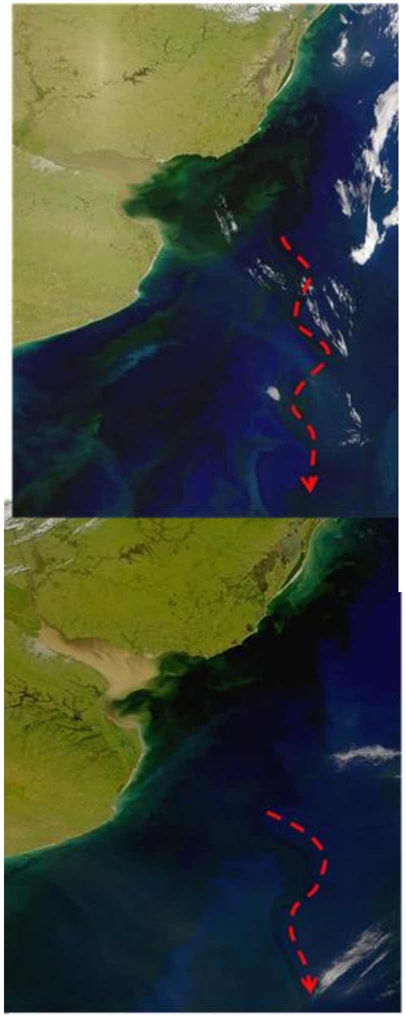

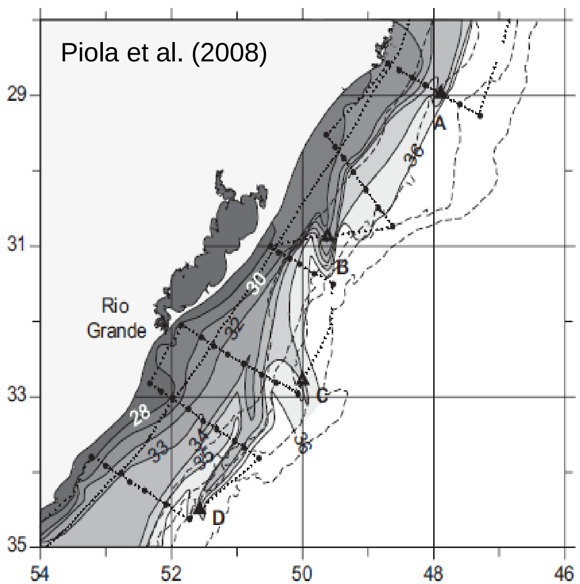

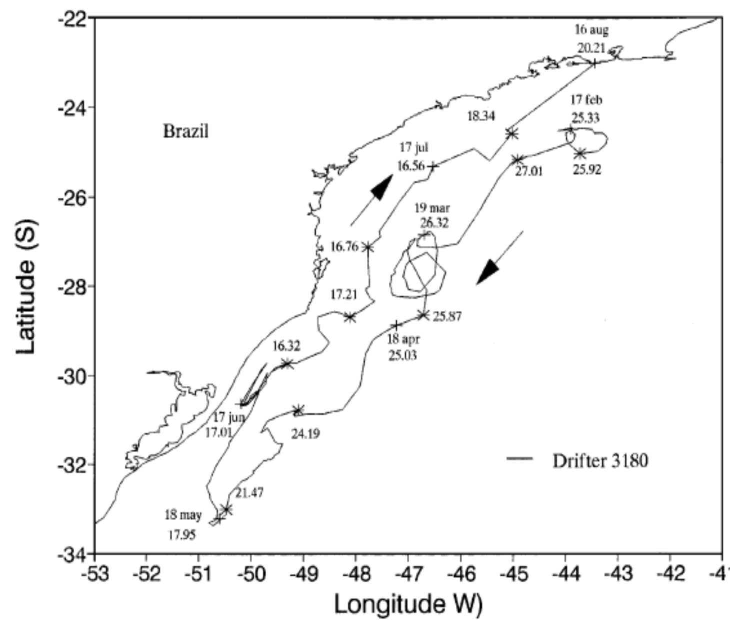

Stevenson et al. (1997)

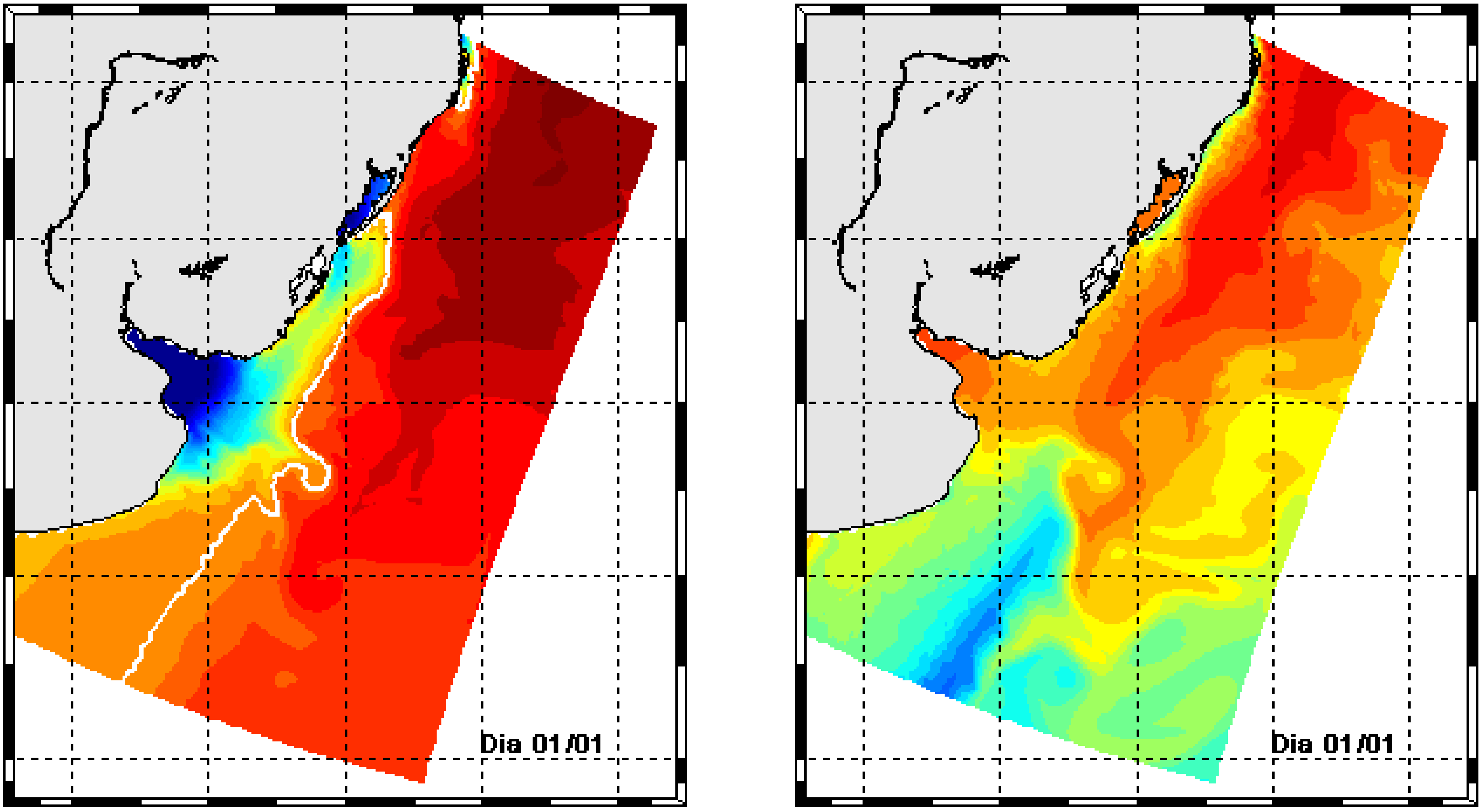

modelo de E. Palma

Frentes de estuário

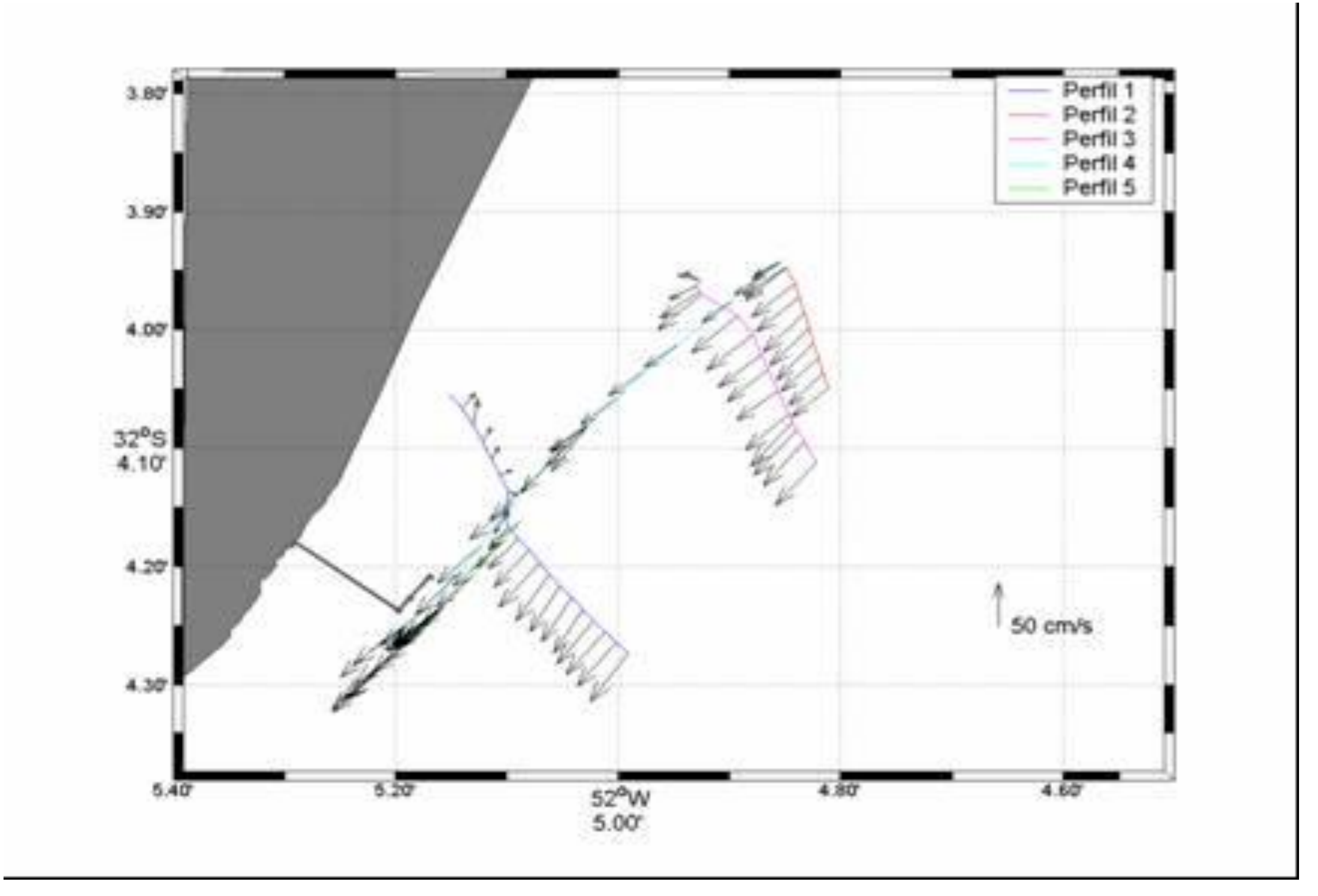

Frentes de estuário

Regime de vazante – ventos de NNE: 13/07/2005

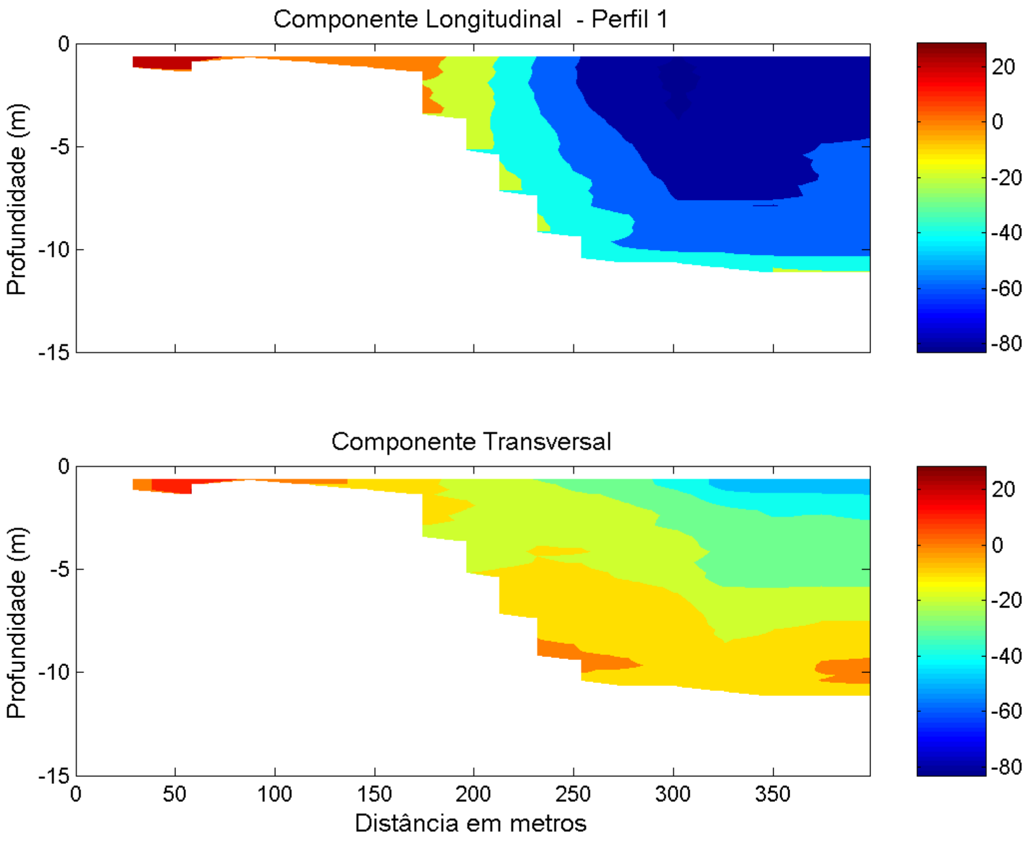

Fig. 17. Linha de espuma formada por diferença de velocidades entre o canal e a parte rasa. A linha acompanha a área onde o empreendimento está previsto

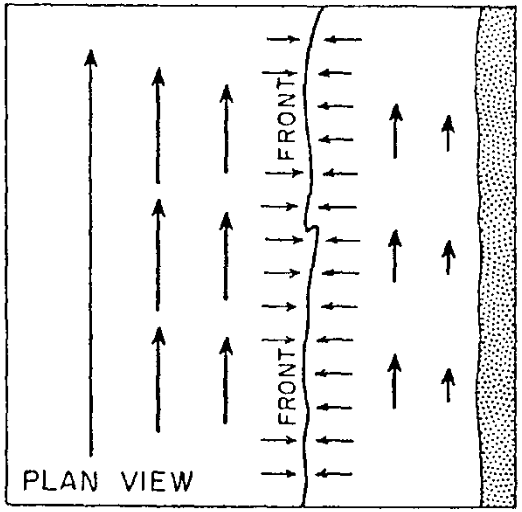

FIGURE 13. Schematic diagram of an estuarine frontal zone. The wiggly lines represent random turbulent motions, and the straight lines tidal currents.[8]

Frente de ressurgência

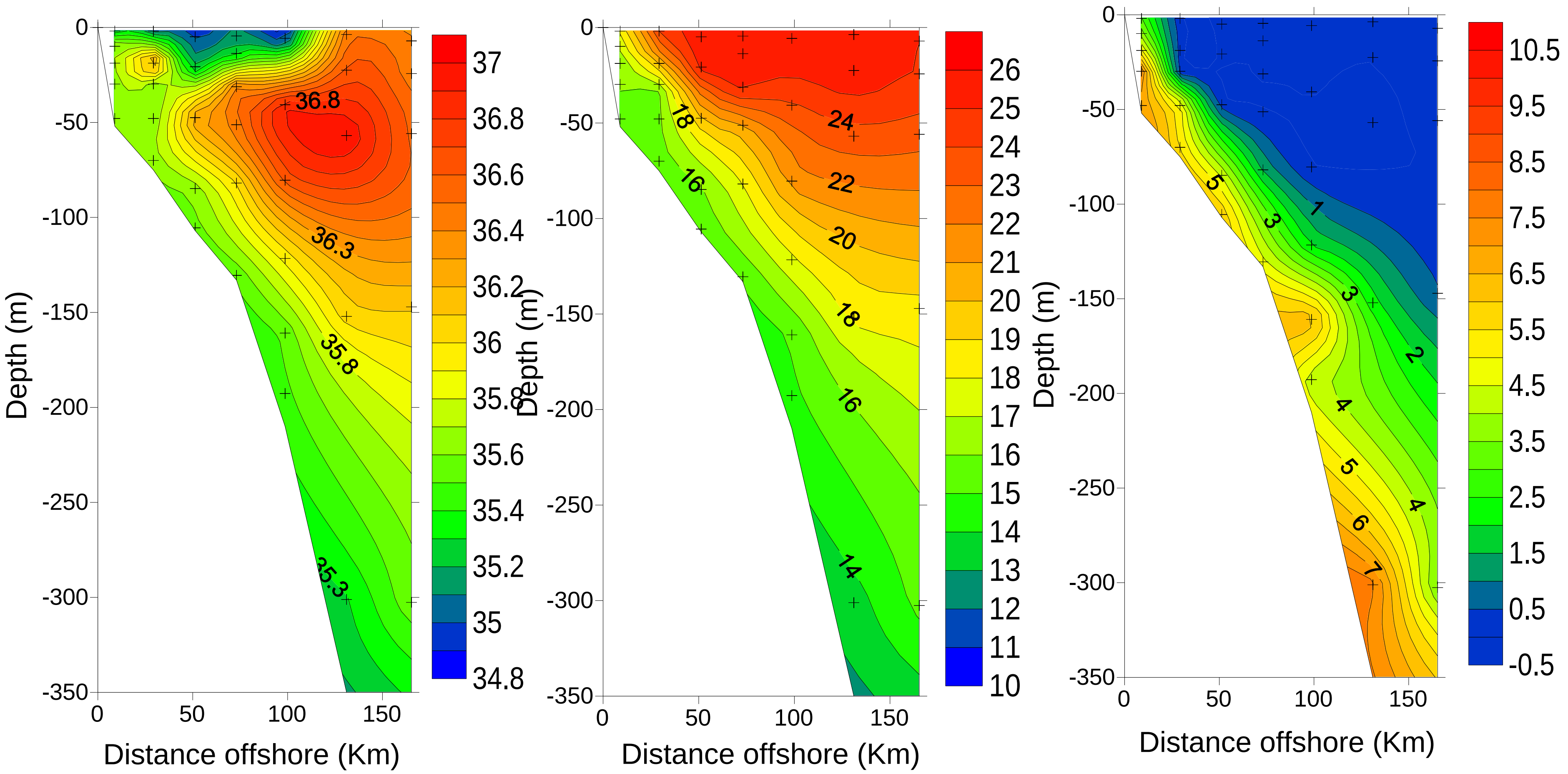

$$\frac{\partial u}{\partial t} + u\frac{\partial u}{\partial x} + u\frac{\partial v}{\partial x} - fv = -\frac{1}{\rho_0}\frac{\partial p}{\partial x} + \frac{\tau_w^x}{\rho_0 h} - \frac{\tau_b^x}{\rho_0 h}$$

$$\frac{\partial v}{\partial t} + v\frac{\partial u}{\partial y} + v\frac{\partial v}{\partial y} - fu = -\frac{1}{\rho_0}\frac{\partial p}{\partial y} + \frac{\tau_w^y}{\rho_0 h} - \frac{\tau_b^y}{\rho_0 h}$$

$$p = \rho_0\left(\frac{\Delta\rho}{\rho_0}g\right)H = \rho_0 c^2$$

$$\tau_w^n = \rho_{ar} C d W_n |W_n|$$

$$\tau_b^y = \rho_0 r U$$

$$\tau_b^y = \rho_0 r \gamma U$$

Equação do movimento

X, u – eixo, componente longitudinal

Y – v eixo, componente transversal

h – profundidade local da pluma. Nos casos em que a pluma toca o fundo h representa a profundidade total

r – coeficiente de fricção representativo da interface externa (fundo) ou interna

y – razão entre o comprimento e a largura da pluma (<1)

U – velocidade longitudinal da pluma determinada a partir de medidas

1586 R. W. Garvine

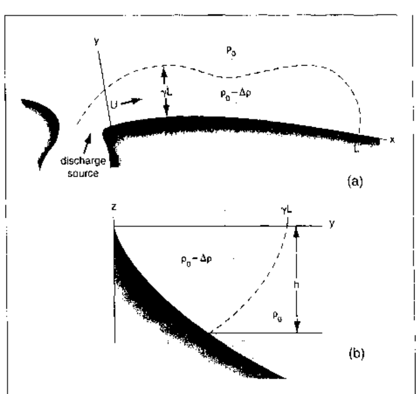

Fig. 1. Defining sketch for buoyant layer scales. (a) x and y are the alongshore and across-shore co-ordinates. Dashed line denotes a typical bounding isopycnal contour for the buoyant layer whose typical density is $\rho_0 - \Delta\rho$. Coastal water has typical density ρ_0. U is the typical alongshore buoyant water velocity, L the alongshore length scale, and γL the across-shore-length scale. (b) A typical across-shore vertical section with vertical coordinate z. Dashed line shows typical bounding isopycnal for the buoyant layer of typical depth h.